

Assessment of the performance of CORDEX-South Asia experiments for monsoonal precipitation over the Himalayan region during present climate: part I

S. Ghimire¹ · A. Choudhary¹ · A. P. Dimri¹

Received: 11 February 2015 / Accepted: 29 June 2015 / Published online: 16 July 2015
© Springer-Verlag Berlin Heidelberg 2015

Abstract Analysis of regional climate simulations to evaluate the ability of 11 Coordinated Regional Climate Downscaling Experiment in South Asia experiments (CORDEX-South Asia) along with their ensemble to produce precipitation from June to September (JJAS) over the Himalayan region have been carried out. These suite of 11 combinations come from 6 regional climate models (RCMs) driven with 10 initial and boundary conditions from different global climate models and are collectively referred here as 11 CORDEX South Asia experiments. All the RCMs use a similar domain and are having similar spatial resolution of 0.44° (~ 50 km). The set of experiments are considered to study precipitation sensitivity associated with the Indian summer monsoon (ISM) over the study region. This effort is made as ISM plays a vital role in summertime precipitation over the Himalayan region which acts as driver for the sustenance of habitat, population, crop, glacier, hydrology etc. In addition, so far the summer monsoon precipitation climatology over the Himalayan region has not been studied with the help of CORDEX data. Thus this study is initiated to evaluate the ability of the experiments and their ensemble in reproducing the characteristics of summer monsoon precipitation over Himalayan region, for the present climate (1970–2005). The precipitation climatology, annual precipitation cycles and interannual variabilities from each simulation have been assessed against the gridded observational dataset: Asian Precipitation-Highly Resolved Observational Data Integration Towards

the Evaluation of Water Resources for the given time period. Further, after the selection of the better performing experiment the frequency distribution of precipitation was also studied. In this study, an approach has also been made to study the degree of agreement among individual experiments as a way to quantify the uncertainty among them. The experiments though show a wide variation among themselves and individually over time and space in simulating precipitation distribution over the study region, but noticeably along the foothills of the Himalayas all the simulations show dry precipitation bias against the corresponding observation. In addition, as we move towards higher elevation regions these experiments in general show wet bias. The experiment driven by EC-EARTH global climate model and downscaled using Rossby Center regional Atmospheric model version 4 developed by Swedish Meteorological and Hydrological Institute (SMHI-RCA4) simulate precipitation closely in correspondence with the observation. The ensemble outperforms the result of individual experiments. Correspondingly, different kinds of statistical analysis like spatial and temporal correlation, Taylor diagram, frequency distribution and scatter plot have been performed to compare the model output with observation and to explain the associated resemblance, robustness and dynamics statistically. Through the bias and ensemble spread analysis, an estimation of the uncertainty of the model fields and the degree of agreement among them has also been carried out in this study. Overview of the study suggests that these experiments facilitate precipitation evolution and structure over the Himalayan region with certain degree of uncertainty.

✉ A. P. Dimri
apdimri@hotmail.com

¹ School of Environmental Sciences, Jawaharlal Nehru University, New Delhi 110067, India

Keywords CORDEX-South Asia · Indian summer monsoon · Himalayas · Precipitation · Bias

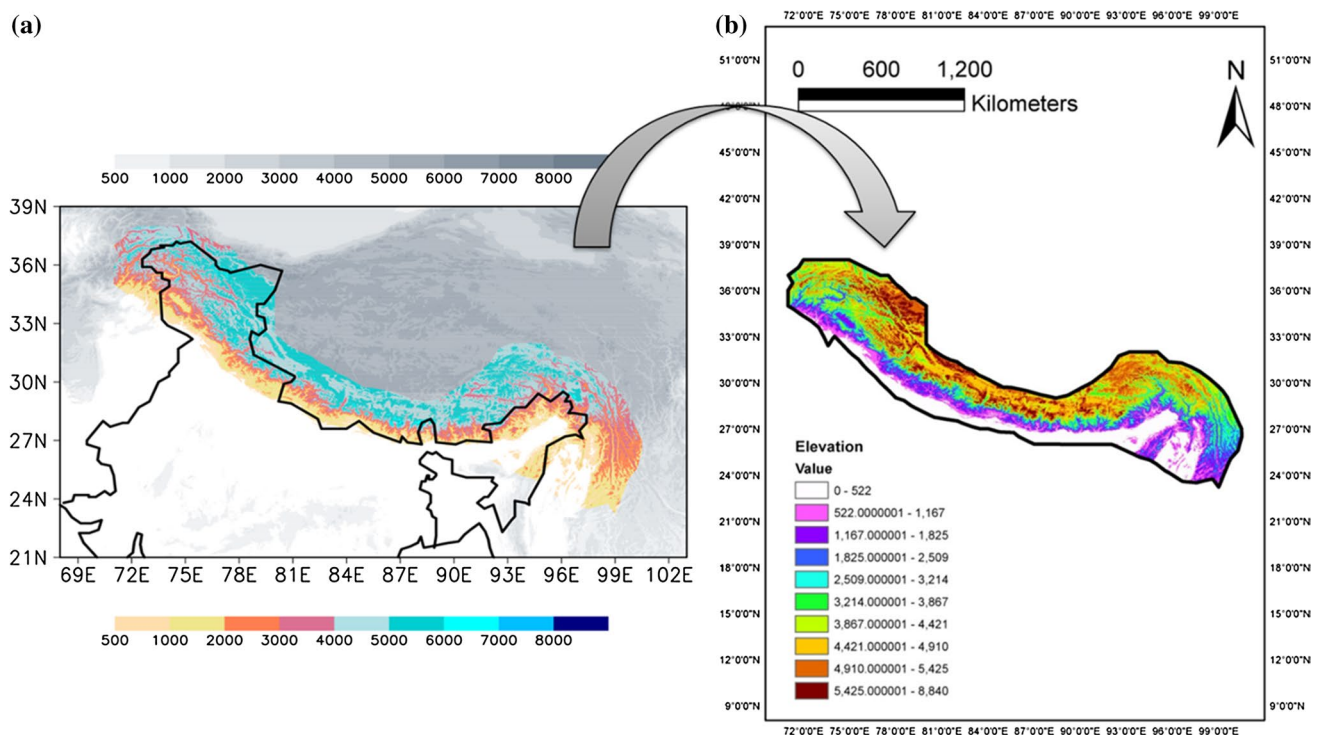


Fig. 1 Topography (m) over **a** Himalayan and Tibetan region (m, grey shaded) and over **b** study area (m, color shaded)

1 Introduction

The Himalayas are the highest chain of mountains forming barrier between the Tibetan plateau in the north and the alluvial plains of the Indian subcontinent in the south (Bajracharya et al. 2007), Fig. 1a. The region consists of high topography reaching more than 8000 m (Kumar et al. 2015). The precipitation pattern and the elevation of the Himalayan region vary as we move from western Himalaya to the eastern and the later increase from south to north as well. In the regions of higher elevations in Himalaya the precipitation is found to vary highly in space up to the scales of tens of kilometers (Anders et al. 2006). The factors such as topography, strength of the moisture-bearing wind, its moisture content and the relief of the range highly affect the amount and intensity of the precipitation, providing enhanced precipitation towards the windward side compared to the leeward (Singh and Kumar 1997; Anders et al. 2006). Topography has a strong effect on the precipitation patterns; the mountains act as a physical barrier and modulate the flow of wind, which disturb the vertical stratification of the atmosphere as well (Dimri 2004; Anders et al. 2006; Dimri 2009; Dimri and Niyogi 2012). Thus the estimation of precipitation, both rainfall and snowfall in this region is a major challenge from scientific and geopolitical viewpoint (Palazzi et al. 2013). Kulkarni et al. (2013) have mentioned that western Himalaya receives precipitation

twice a year, one in the winter months (December–February) due to western disturbances (WD) (Dimri 2004; Dimri et al. 2015) and another in the summer season (June–September) due to Indian summer monsoon (ISM) (Mathison et al. 2013). ISM plays a vital role in marking the beginning of the rainy season for the Himalaya (Fasullo and Webster 2003). The ISM produces more than 80 % of precipitation in the eastern part, whereas as we move to the western part in Northern Pakistan and Afghanistan, it contributes only 30 % (Singh et al. 2011). The WDs delivers heavy precipitation in the western part of the Himalayas (Dimri and Mohanty 2009; Rajbhandari et al. 2014).

The intensity of precipitation during monsoon season decreases as moved from eastern Himalayas to the western, as monsoonal precipitation is normally caused by moist air rising from the Bay of Bengal, striking the mountains on the eastern side and then deflecting and travelling towards the west along the foothills of the Himalayas, thus decreasing the distance from the source of moisture (Singh and Kumar 1997). Kulkarni et al. (2013) and Kumar et al. (2015) have stated that due to lack of proper networks of precipitation station in the mountainous region, enough data cannot be collected for the region, which challenges to prepare the gridded data and it limits the study. The information about the climatological annual precipitation pattern over the Himalaya region is derived and interpolated from the rain gauges, which

themselves are subjected to several kinds of error (Anders et al. 2006). Global climate models (GCMs) operate at a relatively coarse horizontal resolution, thus are not capable of capturing the detailed meteorological processes in the regional scale especially in the area with complex topography (Kumar et al. 2013). They address large-scale climatic features to simulate the atmospheric general circulation at the continental scale satisfactorily (Giorgi and Mearns 1999; Denis et al. 2002; Wang et al. 2004; Giorgi et al. 2009; Rummukainen 2010; Samuelsson et al. 2011; Flato et al. 2013). The dynamical downscaling of GCM simulations has a unique importance over the regions of complex topography (Samuelsson et al. 2011). Dynamical downscaling is used to translate global climate model information down to regional scale to provide more detailed information (Laprise et al. 2008; Rummukainen 2010). Recent studies have shown that RCMs with resolution up to 50–70 km can be integrated over a limited area for a long term simulations with initial and lateral boundary conditions provided by GCMs (e.g. Giorgi et al. 1994). In such regions precipitation is sensitive to horizontal and vertical gradients of topography due to large scale interactions. Regional Climate models (RCMs) are comprehensive and consistent tool with higher resolution, used for dynamical downscaling of the GCM outputs to scales suitable for the end users (Sun et al. 2006a, b; Samuelsson et al. 2011; Rummukainen 2010). RCMs, however are not always useful in understanding the climate of the regions having complex topography, sometimes they show intensified or overestimation of the precipitation over such regions (Hirakuchi and Giorgi 1995), which in this case is the orography (Medina et al. 2010; Samuelsson et al. 2011). Sometimes while simulating the present day climatology, even the internal model processes play an important role in the RCM behavior compared to GCM forcings which may also produce uncertainties in the climatological estimation (Gao et al. 2012). Improved accuracy of precipitation in high resolution simulations can be a good source of input for hydrological and glacier modeling for possible impact studies.

In order to assess the climate change impacts on human and natural systems, the climate change information at the regional to local scale is required, for which a new framework has been initiated, named Coordinated Regional Climate Downscaling Experiment (CORDEX) by World Climate research Programme (WCRP) (Giorgi et al. 2009). So far CORDEX data has not been used and tested to study the seasonal climatology or its performance over the Asian region. Nikulin et al. (2012) and Endris et al. (2013) have performed the assessment of 10 RCMs over the CORDEX Africa domain to evaluated their ability to capture and characterize the rainfall pattern. They have concluded that all the RCMs have simulated the rainfall belt associated

with Intertropical Convergence zone and are able to capture the main features of the seasonal mean rainfall distribution and its annual cycle.

The experiments of CORDEX-South Asia have not been used to evaluate precipitation climatology over the Himalayan region. The objective of this study is to a) assess the performance of the individual CORDEX experiment and their ensemble and b) to analyze and understand the uncertainty present in the simulations and identify the level of agreement between models.

So far, the studies that have been carried out to assess the precipitation climatology of this region have used Tropical Rainfall Measuring Mission (TRMM) satellite imagery, Providing REgional Climates for Impact Studies (PRECIS) etc. (Bookhagen and Burbank 2006; Kulkarni et al. 2013). These studies have used one or few observational datasets (Bookhagen and Burbank 2006, 2010; Palazzi et al. 2013; Kumar et al. 2013, 2015) or model data either GCM or RCM (Palazzi et al. 2013; Kumar et al. 2013, 2015). Study performed by Shi et al. (2011) and Dash et al. (2012) over the part of eastern Himalaya have shown substantial overestimation of the precipitation over the region. Both have used Regional Climate Model 3 (RegCM3) as RCM.

The paper is structured as follows. Section 2 consists of a brief description of study area, about CORDEX and its experiments used for this study, observational datasets used and methodology used for assessing the ability of the experiments in providing precipitation climatology, which includes the process of data handling and a brief description of the statistical analysis applied. Section 3 presents the results which involves a comparative study of the experiments and their statistical analysis. Section 4 presents a summary of the main findings and concludes the paper.

2 Data and methodology

2.1 Study area

The study area includes the great Himalayan Range along with the Hindu-Kush and the Karakoram, Fig. 1a. As it is situated in the tropics, this region is believed to be a hot-spot of climate change (IPCC 2007), but not much detail is known about the climatology of the region (Immerzeel et al. 2009; Shrestha et al. 2000). Bookhagen and Burbank (2010) have shown the major factor of the precipitation in this region to be monsoon, which contributes more than 80 % of the annual precipitation in the central and the eastern Himalaya, including the Tibetan plateau. However, the contribution for the western Himalaya is comparatively less. The study area has been depicted in the Fig. 1. Figure 1a shows the location of the study area, extending from 23° to 39° N and 68° to 103°E, in this figure the study area

is distinguished with the surrounding areas by providing color based on corresponding elevation, covering some parts of 8 countries from Tajikistan to Myanmar, including Afghanistan, Pakistan, India, Nepal, Bhutan and southern parts of China (Palazzi et al. 2013). In Fig. 1b the different elevation of the specific study area is shown with digital elevation, with different colors showing different height of elevation above the mean sea level.

The region under study enwraps high concentration of water and ice as large numbers of glaciers are present in this region (Bajracharya et al. 2007). The region is also referred as water tower of Asia (Immerzeel et al. 2010) and feeds most of the major perennial river systems of the area including the great Brahmaputra, Ganges, Sutlej, Arun and Indus (Bajracharya et al. 2007; Bookhagen and Burbank 2010; Bolch et al. 2012). These rivers provide about 8.6×10^6 m³ of water annually to Central Asia (ICIMOD 2010; WGMS 2008), which is provided in the form of glacier runoff or meltwater during the dry season in monsoonal affected regions. Due to its vast change in topography the region is vulnerable and susceptible to regional changes and impacts and thus needs to be studied for the future impact.

2.2 CORDEX and its experiments

COordinated Regional Climate Downscaling EXperiment (CORDEX) is a program to bring forth regional climate change scenarios globally. It has been sponsored by World Climate Research Programme (WCRP) to direct an international coordinated framework to produce an improved generation of regional climate change projections (Fernández et al. 2010). CORDEX South Asia domain experiment constitutes 11 different suites, with the combination of different RCMs driven by different GCMs' initial and boundary forcings as shown in Table 1 (refer to the table for the name of the experiments that has been used further).

The CORDEX South Asia data was available at a horizontal resolution of 0.44° (~ 50 km) spatial resolution and monthly temporal resolution as well as daily for some experiments. The data of different experiments have been generated by different modeling groups across the world. So they vary in their grid format and structures.

The data for CORDEX South Asia domain was acquired from Center for Climate Change Research (CCCR), Indian Institute of Tropical Meteorology, Pune, India. All the data and the information about the list of experiments are obtained from CCCR website

2.3 Observational dataset

The accurate high resolution rain gauge-based precipitation data are desired to validate the simulation of numerical models and satellite based precipitation data (Turk

et al. 2008). Hence, nowadays, daily gridded precipitation data are highly used to validate the high-resolution climate model simulations, including the extreme events. Xie et al. (2007) developed a high quality gauge based daily precipitation dataset called East Asia (EA) gauge analysis in which an advanced interpolation technique was used to combine the station data from three different sources into one gridded data form. It was applied to correct the bias caused by orographic effects. Andermann et al. (2011) carried an evaluation of precipitation along the Himalayan front and found substantial disagreements among different observational datasets. Existence of such discrepancies makes it difficult in assessing the performance of models.

In present study, for the preliminary comparisons of climatology, three gridded observational datasets have been used (1) Asian Precipitation-Highly Resolved Observational Data Integration Towards Evaluation of Water Resources (APHRODITE) project (version 1003R1, 1951–2007; Yatagai et al. 2009), (2) the Global Precipitation Climatology Center (GPCC) (version 6, 1901–2006; Rudolf et al. 2011) and (3) Climatic Research Unit (CRU) (version 3.0, 1902–2006; Mitchell and Jones 2005). The observational dataset for both GPCC and CRU are monthly precipitation data available at 0.50° spatial and temporal resolution. Whereas, APHRODITE is a daily precipitation data available at 0.25° spatial and temporal resolution developed by collecting rain gauge observations from a number of valid stations ranging from 5000 to 12,000 distributed across Asia (see Yatagai et al. 2009 for number of stations coming in the present study region). The CRU monthly data is based on daily values from rain gauge measurements provided by more than 4000 weather stations distributed around the world (10,000 in 1970s). The GPCC dataset is based on monthly measurement from $\sim 10,000$ stations at the beginning of the twentieth century to more than 45,000 stations in 1986/1987 (see Schneider et al. 2011 for further information about the spatial distribution of these stations) (Table 2).

In situ station data recording in the Himalayan region has a poor spatial coverage and is highly non-homogeneous. The stations are mainly located in the lowland areas and valleys and there is less number of stations over the mountain tops and slopes which are the zones of maximum rainfall. This is a potential source of biased measurement of precipitation towards low elevation regions (Palazzi et al. 2013). Also the different datasets can differ in their recordings due to different number of stations, sensors employing different techniques, different interpolation algorithms used in converting them to gridded form all of which leads to uncertainty in the values of meteorological variables they represent at a point. Besides the uncertainty issue there is also an issue of undercatch of solid precipitation (snow) by

Table 1 List of CORDEX South Asia regional climate model (RCM) experiments

S. no.	Experiment Name	Name used	RCM Description	Driving GCM	Contributing Institute
1	MPI-ESM-LR-COSMO-CLM	COSMO	COnsortium for Small-scale MOdelling (COSMO) model in Climate Mode version 4.8 (CCLM; Dobler and Ahrens 2008)	Max Planck Institute for Meteorology, Germany, Earth System Model (MPI-ESM-LR; Giorgetta et al. 2013)	Institute for Atmospheric and Environmental Sciences (IAES), Goethe University, Frankfurt am Main (GUF), Germany
2	ICHEC-EC-EARTH-SMHI-RCA4	ICHEC	Rosby Centre regional atmospheric model version 4 (RCA4; Samuelsson et al. 2011)	Irish Centre for High-End Computing (ICHEC), European Consortium ESM (EC-EARTH; Hazeleger et al. 2012)	Rosby Centre, Swedish Meteorological and Hydrological Institute (SMHI), Sweden
3	ACCESS-CSIRO-CCAM	ACCESS	Commonwealth Scientific and Industrial Research Organisation (CSIRO), Conformal-Cubi Atmospheric Model (CCAM; McGregor and Dix 2001)	ACCESS1.0	CSIRO Marine and Atmospheric Research, Melbourne, Australia
4	CNRM-CM5-CSIRO-CCAM	CNRM		CNRM-CM5	
5	CCSM4-CSIRO-CCAM	CCSM4		CCSM4	
6	GFDL-CM3-CSIRO-CCAM	GFDL-CM3		GFDL-CM3	
7	MPI-ESM-LR-CSIRO-CCAM	MPI		MPI-ESM-LR	
8	NorESM1-M-CSIRO-CCAM	NorESM		NorESM-M	
9	LMDZ-IITM-LMDZ	LMDZ	Institut Pierre-Simon Laplace (IPSL) Laboratoire de Météorologie Dynamique Zoomed version 4 (LMDZ4) atmospheric general circulation model (Sabin et al. 2013)	IPSL Coupled Model version 5 (IPSL-CM5-LR; Dufresne et al. 2013)	Centre for Climate Change Research (CCCR), Indian Institute of Tropical Meteorology (IITM), India
10	LMDZ-IITM-RegCM4	LMDZ-RegCM4	The Abdus Salam International Centre for Theoretical Physics (ICTP) Regional Climatic Model version 4 (RegCM4; Giorgi et al. 2012)	IPSL LMDZ4	CCCR, IITM
11	GFDL-ESM2M-IITM-RegCM4	GFDL-ESM2M	ICTP RegCM4	Geophysical Fluid Dynamics Laboratory, USA, Earth System Model (GFDL-ESM2M-LR; Dunne et al. 2012)	CCCR, IITM

Table 2 Precipitation trends (mm/day/year) in the study during summer (JJAS) for the experiments, ENS and APH

S. no.	Experiments	b (slope parameter, regression coefficient)	Standard error	t-ratio	p-value (significance)
1	ACCESS-CSIRO-CCAM	-0.025	0.013	-1.864	0.071
2	GFDL-CCM3-CSIRO-CCAM	-0.021	0.014	-1.573	0.125
3	CCSM4-CSIRO-CCAM	-0.018	0.011	-1.643	0.11
4	CNRM-CM5-CSIRO-CCAM	-0.013	0.011	-1.165	0.252
5	GFDL-ESM2M-IITM-RegCM4	0.003	0.008	0.405	0.688
6	LMDz-IITM-LMDz	0.027	0.017	1.554	0.129
7	LMDz-IITM-RegCM4	0.007	0.005	1.521	0.137
8	MPI-ESM-LR-CSIRO-CCAM	-0.003	0.014	-0.189	0.851
9	ICHEC-EC-EARTH-SMHI-RCA4	0.012	0.011	1.09	0.284
10	Nor-ESM1M-CSIRO-CCAM	-0.015	0.012	-1.224	0.229
11	COSMO-CLM	-0.013	0.012	-1.06	0.297
12	ENSEMBLE	-0.005	0.003	-1.605	0.118
13	APHRODITE	-0.006	0.008	-0.834	0.41

the station sensors due to the effect of wind (Rasmussen et al. 2012).

Andermann et al. (2011) carried out a comparative analysis of various gridded precipitation datasets both remote sensing based satellite dataset and interpolated rain gauge dataset including the ground based observations and studied the applicability of these datasets over the Himalayan region especially for the regions where the topography has a pronounce effect on precipitation. He found discrepancies between the datasets over these regions. Palazzi et al. (2013) compared satellite observations (TRMM 3B42), station data interpolated onto a regular grid (APHRODITE, Global Precipitation Climatology Centre (GPCC), and Climate Research Unit (CRU) datasets), merged satellite and rain gauge data (Global Precipitation Climatology Project (GPCP) climatology), reanalyses dataset (ERA-Interim) over the Hindu Kush Karakoram and Himalayan region. Consistent with the findings of Palazzi et al. (2013) and Andermann et al. (2011), Mishra (2015) also found that observational datasets show considerable uncertainty in the foothills of the Himalaya. APHRODITE (hereafter referred as APH) was further used for the comparison of performance of the experiments. The vertical interpolation of the APH data is important for the study of precipitation in complex topography such as Himalayas where there is sudden increase in the elevation. The qualities of gridded datasets have always been under scrutiny due to their coarser resolution and the products of APH are no exception. Andermann et al. (2011) have recently evaluated APH data with rain gauge and five other gridded datasets including TRMM precipitation data for Nepal Himalaya and found that APH data provides a good temporal variability on a monthly to annual scale and even in some cases the daily variations. The use of APH data has been increasing rapidly

for precipitation analysis as done by Dimri et al. (2013) and Mathison et al. (2013).

2.4 Methodology

As discussed earlier, at the beginning of this study the performance of the individual experiments is analyzed and then the uncertainty in these experiments is studied. For the evaluation of the precipitation climatology, at first the time period was selected based the availability of the data for each CORDEX experiments. Few experiments were having the present climate data from 1950 to 2005 and rest have only from 1970, thus for the convenience of the study the common time period of 1970–2005 was chosen. Since the RCM data used in this study were produced by different modeling groups and centres across the world therefore to bring all the datasets including the observational dataset into a common data format, same grid structure as well as same resolution, so as to use them for inter comparison and other analytical procedures Climate Data Operators (CDO)—a climate data post-processing tool (Schulzweida et al. 2006) was used. Same tool has been used for masking out the study region from original CORDEX files which is over South Asia. The study region consists of 2367 grid points.

The monsoon period, from June through September was chosen for this study as it is the dominant period of precipitation throughout the study region (Kulkarni et al. 2013). The comparison between the observed and simulated seasonal mean precipitation climatology over the region is done to examine the ability of the experiments to capture the long-term mean spatial distribution of precipitation. The annual cycle of the precipitation averaged over the study area (shown in Fig. 1), has been studied to assess the simulation of precipitation seasonality by the experiments.

Furthermore, a few statistical techniques have been used to aid in better comparison of climatology–spatial correlation (Pearson correlation coefficient; Hall 2015) between experiments and observations have been calculated for each year from 1970 to 2005 to assess the consistency of the models in representing the spatial distribution of precipitation with time (year). Besides this, temporal correlation (Pearson correlation coefficient) between observed and simulated yearly (JJAS mean) precipitation values is also calculated at each grid point to see the spatial consistency in capturing the precipitation variability over time.

To see the ability of the experiments how well they represent the observed change of precipitation over time—yearly variation in seasonal mean precipitation (as time series of area averaged precipitation over the study region) is analyzed in comparison with observation. Furthermore, for better understanding this aspect of model ability an analysis of the spatial distribution of standard deviation of the 36 years JJAS mean precipitation has been studied. Thirdly, trend analysis has also been carried out to further explore the ability of model to simulate the temporal variability in precipitation. This also gives an insight into how models vary in simulating the trends in response to various external forcings (Giorgi et al. 2004) and also their inter-annual modes of internal variability. We apply least square linear regression method to estimate the slope of the JJAS mean precipitation trend at each grid point in our study area over the period of 36 years (1970–2005) representing the present climate and see the pattern of its spatial distribution over the study area. Secondly, *t* test at 5 % significance level has also been applied over the spatially averaged precipitation values (time series) for the same period to determine the significance of the trend i.e., whether the slope is significantly different from zero i.e., the null hypothesis is that the slope is zero. This is inferred from the *t*-ratio (or *p* value) which is the ratio of the slope or regression coefficient to its standard error. If this ratio is greater than two (or *p* value <0.05) then the null hypothesis is rejected and the slope or trend is considered to be significant (Wilks 2011).

The Taylor diagrams provide a graphical summarization of how closely models or experiments' behavior resemble the observation (Taylor 2001). The similarity/difference between the experiments is quantified in terms of their correlation, their centered root mean square (RMS) difference and the amplitude of their variations represented by their standard deviation (Taylor 2005). It is used to evaluate the spatiotemporal pattern errors in the experiment results (Taylor 2001). In a Taylor diagram, the distance from the origin is equal to the standard deviation, while the distance from the reference or the APH is the RMS difference and the cosine of the polar angle is equal to the correlation. If any experiment would have no error as compared to RMS, it would perfectly correlate with the APH, having the same

standard deviation. In order to identify the strengths and the level of uncertainty in the experiments, the inter-experiment spread was examined. The spread among experiments was calculated as the standard deviation of 36 year mean of individual experiments with respect to their ensemble.

Similarly, to assess the capability of the experiments in representing the variability of monthly precipitation, the evaluation of frequency distribution as gamma distribution was carried out. The gamma distribution is a common choice for the data that are bounded on the left by zero, i.e., they cannot be less than zero e.g. precipitation distribution (Wilks 2011). The gamma distribution consists of two major parameters α , the shape parameter and β , the scale parameter and the third parameter, μ which is the location parameter. The distribution takes on a wide variety of shapes, which depends on the shape parameter. And the stretch of the curve is determined by the scale parameter. Higher/Smaller the scale parameter more the curve is stretched/squeezed.

In addition, the scatter plot is also generated which helps in understanding how closely the precipitation amounts for the experiment matches with the observation over the spatial range of precipitation values.

3 Results and discussion

Figure 2 shows the monsoonal precipitation climatology (JJAS) for the time period of 1970–2005 over the study area from the 3 observational datasets, APH, GPCC and CRU. Among these datasets, APH captures precipitation climatology in the range from 0.5 to 27 mm/day. As the topography and terrain plays an important role in the occurrence, releasing and enhancing of the convection processes, the sharp rise of the Himalayas from the Ganges and Indus plains cause the maximum precipitation to occur in this region (Medina et al. 2010). The transport of the moisture-laden monsoon clouds from the eastern to the western Himalaya causes more precipitation in the eastern Himalaya compared to the western, which is seen in model simulated precipitation as well. On comparison, it is seen that APH represents more spatial information on precipitation climatology than GPCC and CRU over the study region (Fig. 2a), as it is able to capture the well known features of precipitation in this region with a clear band of higher precipitation along the southern rim of the Himalayas extending up to north-east India and the general smaller precipitation as we move towards the west. Among 3 datasets CRU showed comparatively smaller precipitation, Fig. 2c. The finer resolution of APH compared to other datasets have helped in capturing precipitation climatology, hence producing better result. However, the highest amount of precipitation is captured in the eastern Himalaya, when

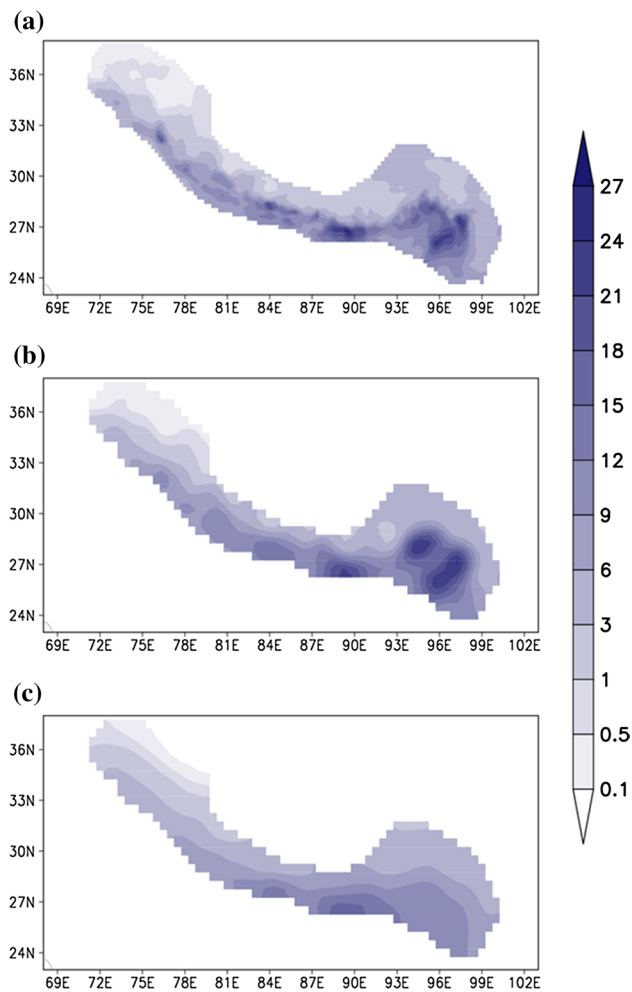


Fig. 2 Observed JJAS precipitation (mm/day) climatology during 1970–2005 over the study area as shown in Fig. 1b in **a** APHRODITE, **b** GPCP and **c** CRU

we look at the other two observational dataset, APH and GPCP. Also the moist, vegetated land surface in the eastern Himalaya and the Ganges–Brahmaputra delta shows the substantial amount of precipitation in this region compared to relatively barren land in the western region (ICIMOD 2010). In view of the better representation of horizontal and vertical algorithmic gradients and reporting of station densities during the preparation of the regridded data set, APH was chosen for further analysis and the comparisons (Yatagai et al. 2009; Krishnamurti et al. 2009).

The annual cycle of simulated annual precipitation of the 11 CORDEX experiments, their ensemble (hereafter called ENS) and corresponding APH observation averaged over the study region during the study period is shown in Fig. 3a. In general, the spread among the experiments is large throughout the year, however for August the experiments show less spread. The spread among the experiments show larger amplitude than that of the observation.

Least amount of simulated precipitation (0.71 mm/day) is shown in the month of January by ICHEC and maximum precipitation (11.8 mm/day) in the month of June is shown by MPI. Whereas, ENS shows maximum precipitation (8.31 mm/day) in the month of May and minimum precipitation (2.4 mm/day) in the month of December. Similarly, Fig. 3b shows the precipitation cycle for monsoonal months (JJAS) only. In both Fig. 3a and b, the simulation of six experiments which have used CSIRO-CCAM as the downscaling RCM shows wet bias and follow similar precipitation pattern showing the shift of distribution of the seasonal precipitation with higher order. Among all the experiments, ICHEC shows closest resemblance with the observation in simulating the annual cycle curve. ICHEC outperforms ensemble as well, as the latter's performance is negatively affected by the other experiments. ICHEC shows similar pattern of precipitation as in the corresponding APH observation, former showing the maximum monthly average precipitation of 8.17 mm/day and that of the latter is 7.11 mm/day in the month of July. In case of minimum monthly average precipitation, ICHEC shows 0.71 mm/day in January but APH shows 0.39 mm/day in December. Almost all the experiments show an overestimation of precipitation throughout the year. However, two experiments LMDZ-RegCM4 and GFDL-ESM2M using RegCM4 as a downscaling RCM show precipitation in the range of 1.77–5.14 and 2.49–5.13 mm/day respectively, which in average is smaller than the corresponding APH observation. The experiment LMDZ also follows similar pattern of precipitation as APH, ranging from 0.94 to 8.85 mm/day, but we have chosen only ICHEC as it shows overall precipitation magnitudes and patterns in closer proximity with the observations (the statistical method for choosing this experiment is discussed further in Fig. 7d). Due to such a high variation in the value of the precipitation in the experiments, the precipitation seasonality of the ENS is captured poorly. On comparison it is seen that all the experiments show peak monthly average precipitation during monsoon season, i.e., June to September with lead and/or lag of a month dominates within themselves.

Figure 4 shows JJAS precipitation climatology over the study region for the time period of 1970–2005 in 11 experiments (Fig. 4a–k) and in their ENS (Fig. 4l). Most of the experiments capture spatial distribution of model precipitation fairly well expect for GFDL-ESM2M, LMDZ and COSMO-CLM in Fig. 4b–d. In these cases much less precipitation is seen. However, the former two show less precipitation throughout the study region, whereas the latter shows comparatively higher precipitation in some parts of eastern Himalaya. As seen in Fig. 4j ICHEC shows better precipitation climatology among all the other experiments as compared with the corresponding observation (Fig. 2a). This is also one of the reasons that ICHEC experiments is

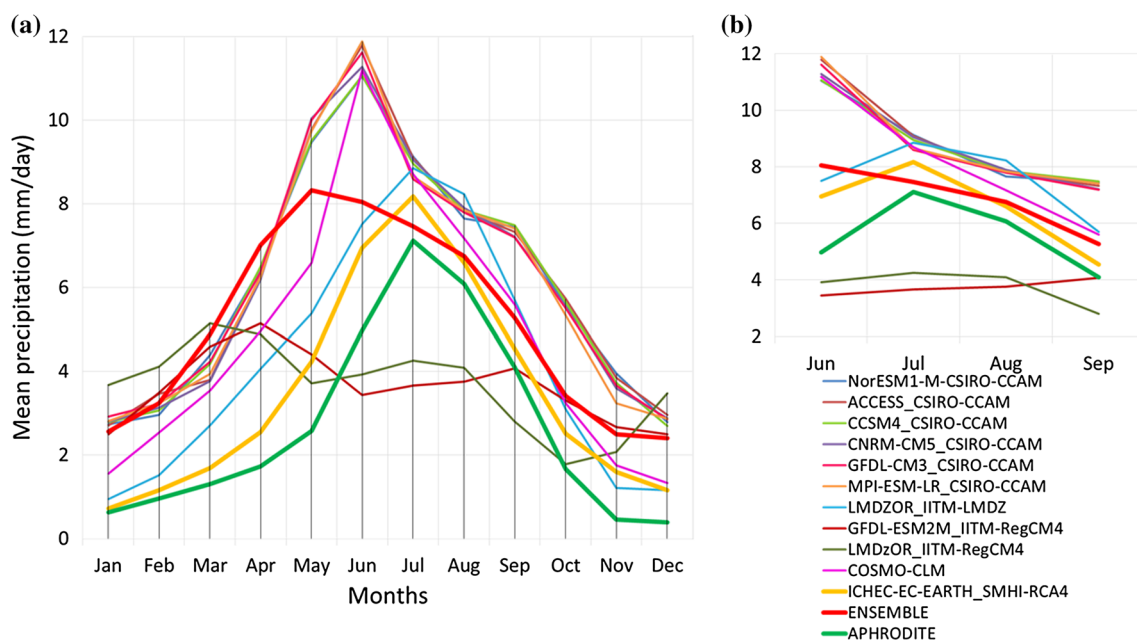


Fig. 3 **a** Mean annual cycle of precipitation (mm/day) over the period of 1970–2005 and **b** monsoon months (JJAS) precipitation cycle from the 11 CORDEX experiments, their ensemble and corre-

sponding observation. Nomenclature given in Fig. 3b corresponds to the respective CORDEX experiment as described in detail in Table 1

thus chosen for the further discussion/analysis. The simulation of seasonal mean precipitation fields are also depicted in bias term in all the experiments with corresponding APH observations over the study region for the given time period and are shown in Fig. 5. The precipitation bias is showing wide variation in their spatial distribution in individual experiments. All the 6 experiments using CSIRO-CCAM (Fig. 5a, e–h, k) as the downscaling RCM experiment show dry bias along the foothills of the Himalayas and wet bias over the higher elevation regions. This could be due to shortcomings in the model physics in representing the various microphysical processes associated with the formation of hydrometeors, its advection, formation of cloud and fall out of precipitation. For example if the model atmosphere is too stable or the flow is not strong enough the air may not ascend over the mountain range and the flow is blocked and precipitation is less over the foothills of mountains. This blocked air tends to find its path causing further ascend windward of the mountain range and can enhance lifting and precipitation further up (Roe 2005). The dry bias along the foothills and wet bias in the high elevations could also be due to the inherent nature of observational dataset itself as there is a sparse presence of observation stations in the higher reaches of the Himalaya compared with the lower elevation regions. Andermann et al. (2011) concludes that there is a potential underestimate of precipitation at high elevations because there are no observation sites here. Similar kind of distribution is seen in the COSMO-CLM experiment (Fig. 5d). Whereas, overall ICHEC shows smaller

bias as compared to other experiments, Fig. 5j. It indicates that it performs better over other experiments. Especially, over the western Himalayas, ICHEC and LMDZ show very close resemblance with corresponding observation showing bias to be not more than 1 mm/day. As discussed earlier, GFDL-ESM2M and LMDZ shows dry bias as simulating much less precipitation. Higher precipitation in the leeward side of the mountains may be resulting in the typical precipitation pattern observed in the LMDZ model. This could be due to the model response to sharp variations in elevation. A convergence zone may be getting created if a narrow range of mountain exists so that when air flows over these regions it splits around the mountain and converges in the leeward side where ascent occurs causing precipitation (Mass 1981).

Due to the sharp gradients of topography from the Ganges and Indus plains all the experiment seems to produce less precipitation over the foothill and lower elevation region hence showing dry bias and produce higher precipitation over the higher elevation region hence showing wet precipitation (refer to Fig. 1b). These different orographic interactions represented within the model physics and dynamics led to different precipitation mechanism (Dimri and Niyogi 2012).

Figure 6 shows the variation of precipitation distribution of the observation with the elevation. The gridpoint precipitation values coming in the study area averaged over the 36 years period (1970–2005) is shown in the form of scatter plot. Here, the number of grid points falling within

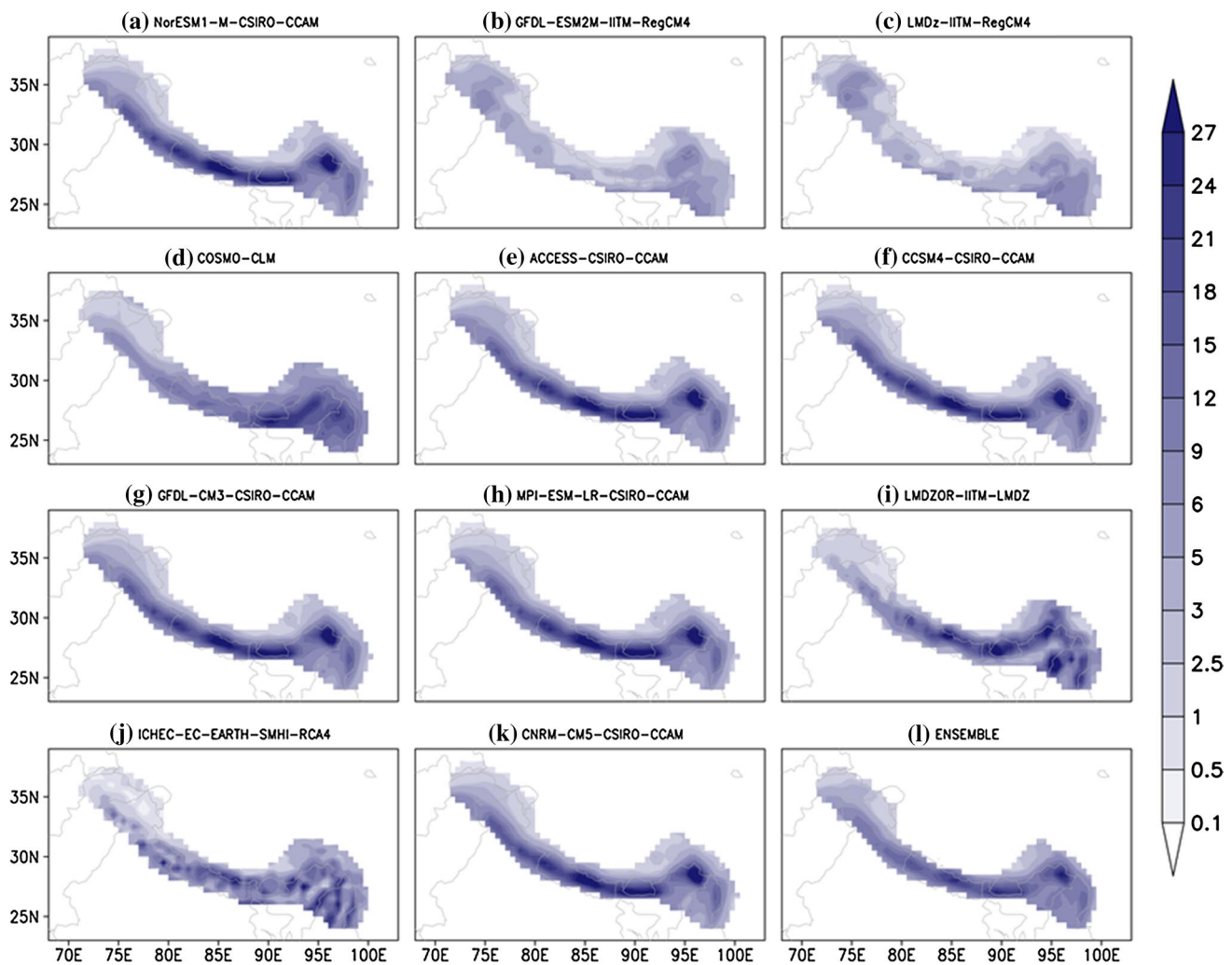


Fig. 4 JJAS precipitation climatology (mm/day) for 1970–2005 of the 11 CORDEX experiments (a–k) listed in Table 1 and their ensemble (l)

each 1000 m of increasing altitude is also shown to give a quantitative idea of topography distribution. In the lower elevations, we can see that there is a considerable spread in the precipitation which means lower elevation shows more spatial variation in the amount of precipitation possibly because of the enhanced role of sharp orographic changes at the lower elevations on the convection and cloud formation processes resulting in varying precipitation mechanisms spatially. As we go to the higher elevations the spatial variability reduces significantly (as seen by smaller spread in the dots) as well as the precipitation is of low magnitudes of up to 5 mm/day above 4000 m. This seems to be a realistic representation of mountain environment by the APH dataset as by the time the cloud reaches the higher altitudes of mountains it gets devoid of most of its moisture due to its fallout as precipitation in the lower elevations. So the precipitation amounts are low in almost all the regions of higher elevation and they are similar in magnitudes. The

less difference in magnitudes between different elevations may be due to similar shapes and orientation of the peaks thus the precipitation forming processes may follow similar path. In our study region spatially the topography is mainly distributed between 4000 m and 5000 m elevations. Though about 26 % of total grid points are present between 4000 m and 5000 m elevations compared to 23 % in regions with elevation up to 1000 m but the later shows relatively higher percentage of total precipitation as the precipitation in the lower elevations are higher. This indicates that most of the precipitation in the Himalayan region is concentrated in the lower elevations.

Figure 7 shows the distribution of precipitation bias (with APH) at grid points with elevation to understand how the model's behavior or ability to capture the observed precipitation varies with the elevation. Here we can see that in general all the experiments at above 3000 m elevation show smaller bias as well as smaller spatial spread

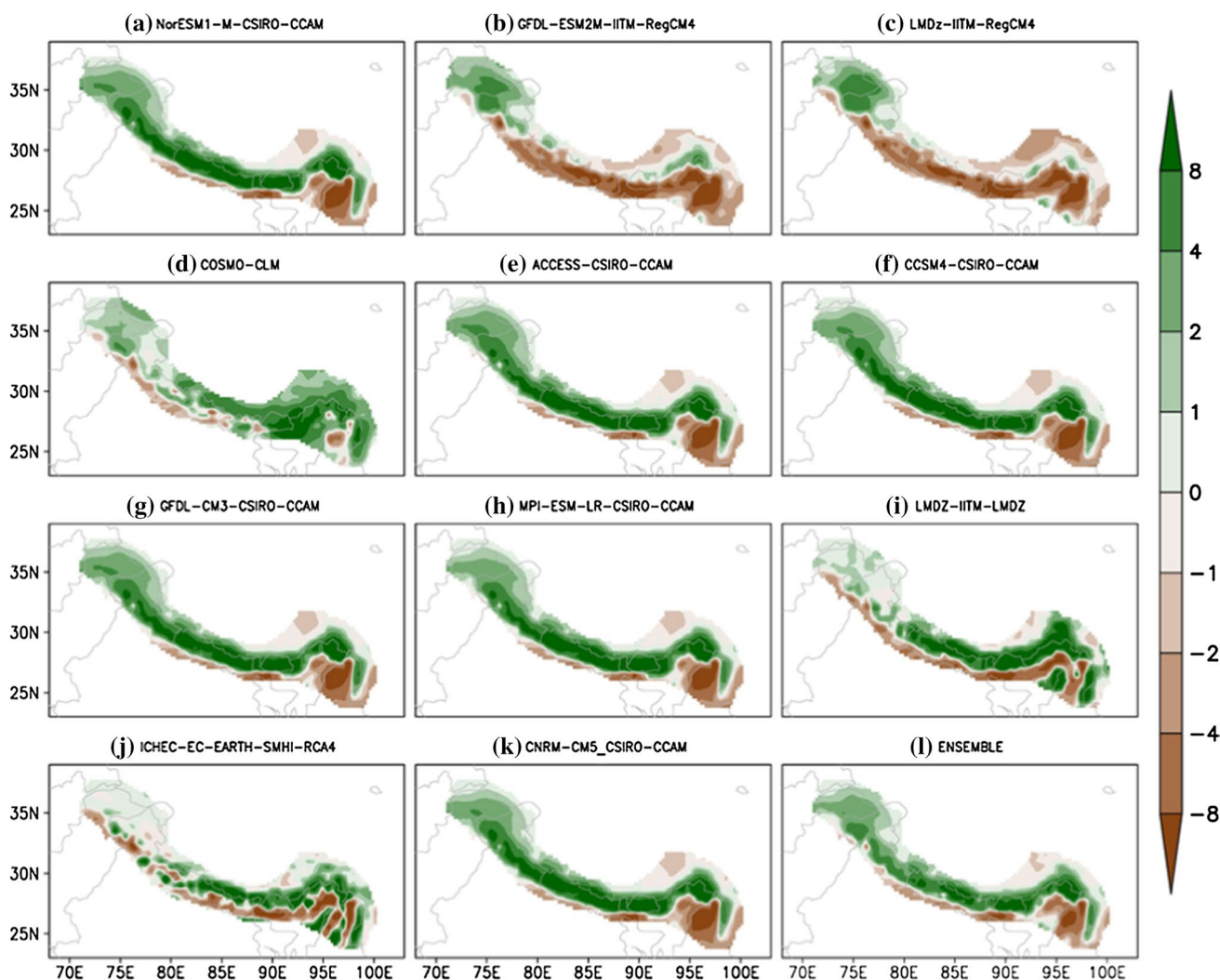


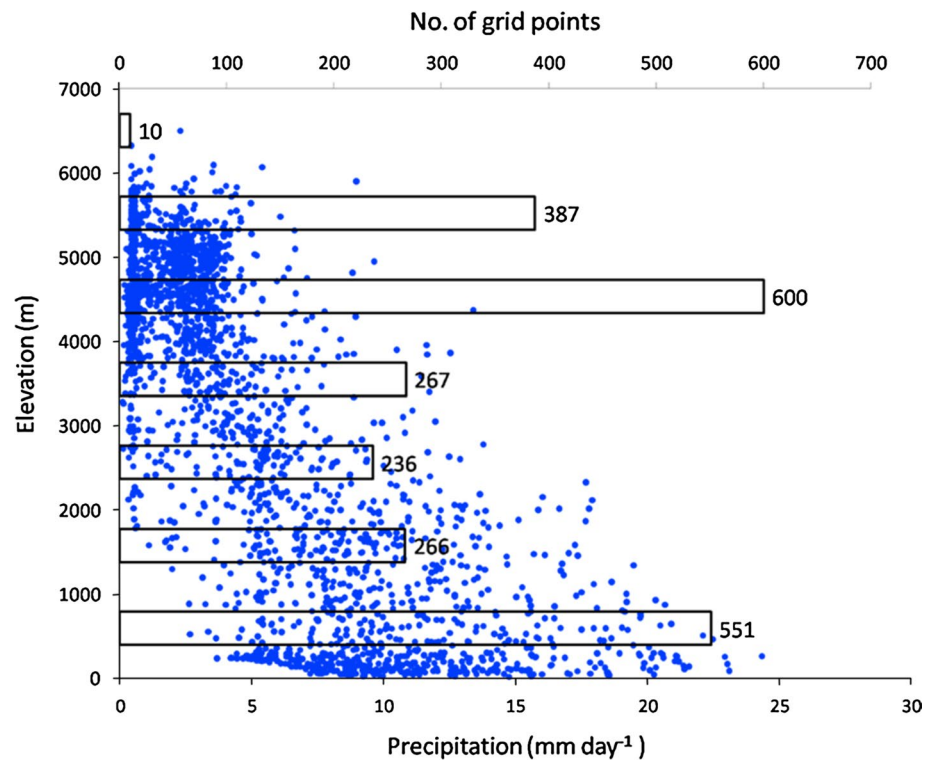
Fig. 5 Same as Fig. 4, but precipitation bias (mm/day)

in the precipitation. The smaller spatial variability at high altitudes is similar to what we found in the observation (Fig. 6). This means that model physics aided by finer representation of topography which is an inherent quality of RCMs is together working well in capturing high altitude processes associated with the formation or fallout of precipitation at such heights. Interestingly at lower range of elevation below 3000 m the experiments tend to show dry bias especially GFDL-ESM2M and LMDZ-RegCM4 which prominently shows this behavior. For these experiments which show dry bias at lower elevations and closer resemblance with observation at higher elevations may be related as the precipitation seems to be underestimated overall for this region.

Figure 8 shows yearly variability of precipitation for APH and each experiment along with ENS in terms of standard deviation in the 36 years values of JJAS mean precipitation at each grid point in the study area. The

experiment, GFDL-ESM2M (Fig. 7c), LMDZ-RegCM4 (Fig. 7d) and ICHEC (Fig. 7k) comparatively show less standard deviation. This result shows that the year-wise seasonal mean precipitation values of fore mentioned experiments do not disperse much from the long-term seasonal mean at each grid point. Whereas, all the other experiments show higher standard deviation particularly over the eastern Himalayan region. However, on contrary to individual experiments their ENS show smaller standard deviation. The earlier works on the long-term precipitation distribution pattern and their trend for the Himalayan region includes studies by Pant and Borgaonkar 1984; Pant et al. 1999; Shrestha et al. 2000; Sharma et al. 2000; Singh and Sen Roy 2002; Kumar et al. 2005; Fowler and Archer 2006. In some of these studies, positive trends (increasing seasonal or annual mean precipitation) have been reported in the precipitation pattern for some localized regions such as Sharma et al. (2000) for Kosi basin in Nepal and

Fig. 6 Variation in the observed precipitation (mm/day) with elevation



Kumar et al. (2005) for the state of Himachal Pradesh in India; while on the other hand negative trends have been found for other places like Singh and Sen Roy (2002) for Beas basin and Kumar and Jain (2010) for Qazigund and Kukarnag which comes in Kashmir. Interestingly, some studies are also available where no significant trend of precipitation was found, such as Archer and Fowler (2004) for upper Indus basin; Khan (2001) for Jhelum basin region in Pakistan and Joshi et al. (2014) for Almora and Nainital stations of central Himalayan region in India. But such localized studies cannot represent the trend of ISM for the entire Himalayan region as monsoon is a regional phenomena and for Himalayan region which consists of complex and sharply varying terrain features precipitation also varies from one place to other place. So, in this section we have investigated long-term trend of JJAS mean precipitation over the period of 36 years (1970–2005) for our study area representing a spatial domain over Himalaya which includes the places studied earlier. We examine the simulated trends in comparison with that of APH observation to see the ability of the experiments to represent the observed change of precipitation over time. This can also give us an insight into how models vary in simulating the trends in response to various external forcings (Giorgi et al. 2004) and also their interannual modes of internal variability. We apply least square linear regression method to estimate the slope of the trend and see its spatial distribution over the study area. Secondly, *t* test has also been applied over the

area averaged precipitation values to determine the significance of the trend i.e. whether the slope is significantly different from zero.

A noticeable feature observed in the APH (see Fig. 9a) is the drying (negative trend) JJAS mean precipitation of up to 0.05 mm/day/year over south western part of the study area near Myanmar and an increasing trend of as high as over 0.1 mm/day/year in eastern Himalaya. In the previous figure Fig. 8a also it was seen that APH over this region is showing high variability over the years which confirms this finding. The increasing trend may be the result of a combination of several factors like forcings by greenhouse gases, aerosols, land-use changes etc. during the period (1970–2005) or it may be due to the natural variability of the climate system from year to year. The Karakoram region also shows a slight positive (increasing) trend of mostly around 0.02 mm/day/year. The western Himalaya show a decreasing trend of precipitation while the central Himalayan region show a mixed spatial distribution of trend from positive to negative values. Negative precipitation trends in parts of western Himalaya have been reported by others, like Singh and Sen Roy (2002) for Beas basin and Kumar and Jain (2010) for Qazigund and Kukarnag which comes in Kashmir. Trend analysis of the spatially averaged time series for the 36 years period of APH precipitation shows that overall, the Himalayan region considered in the present study shows decreasing trend of monsoonal mean precipitation (0.006 mm/day/year) though this trend is not

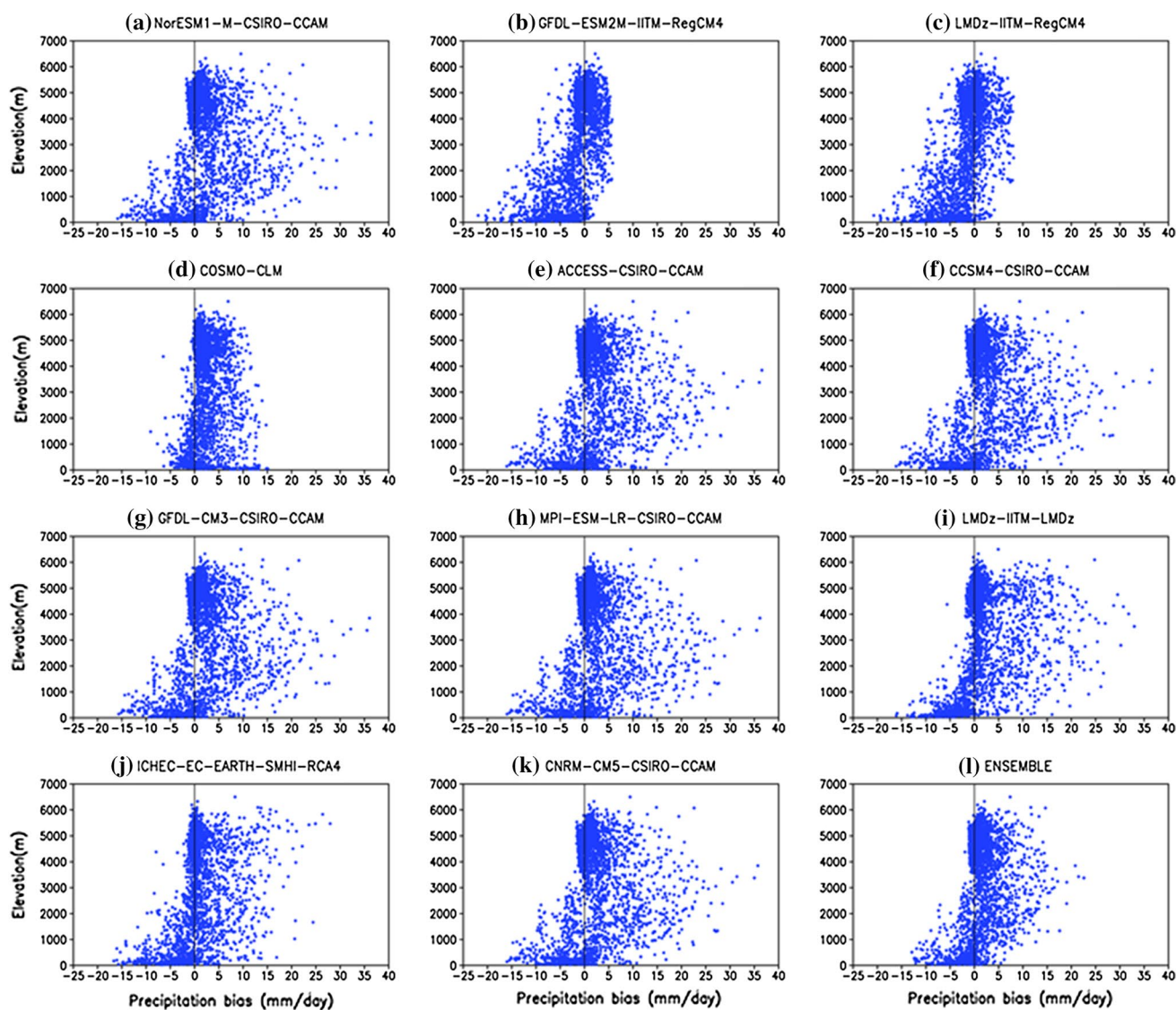


Fig. 7 Variation of precipitation bias (mm/day) with elevation for the experiments and ENS

significant (p value >0.05). Mukherjee et al. (2014) based on APHRODITE data also reported that trends are not significant for most of the Himalayan region. A significantly decreasing trend was also found by Palazzi et al. (2013) over Himalayan region in the APHRODITE dataset for 1951–2007 period.

In Fig. 9b–m the distribution of trend of the 11 CORDEX experiments and their ensemble mean is presented. The results from variability analysis in Fig. 8 and trend distribution in space support each other as we can see that the areas in the study region where there is a high variability (Fig. 8b–m) over the 36 years show a high value in their trend also which is natural. For e.g. two experiments GFDL-ESM2M and LMDZ-RegCM4 (Fig. 8c, d respectively) show much less variability and hence the calculated trend over this period also comes out to be less in these

experiments (Fig. 9c, d respectively). As we can see that like in the case of climatology (Fig. 4) and variability in 36 years (Fig. 8) of JJAS mean precipitation the experiments are showing uncertainty between them in simulating its trend also. This could be due to the differences in the model physics of the experiments which simulate the convection processes that may be resulting in varying yearly magnitude of seasonal mean precipitation in different experiments ultimately resulting in disagreement in the trend simulation. Talking individually about experiments we find 5 of the 6 experiments in which CCAM RCM has been used (in Fig. 9 b, f–h, l) show predominantly a decreasing precipitation trend in the eastern Himalayan region as found in observation also (for a smaller region) though a disagreement is seen for other regions in the same experiments. While in the other CCAM experiment MPI (Fig. 9i) and LMDZ (Fig. 9j)

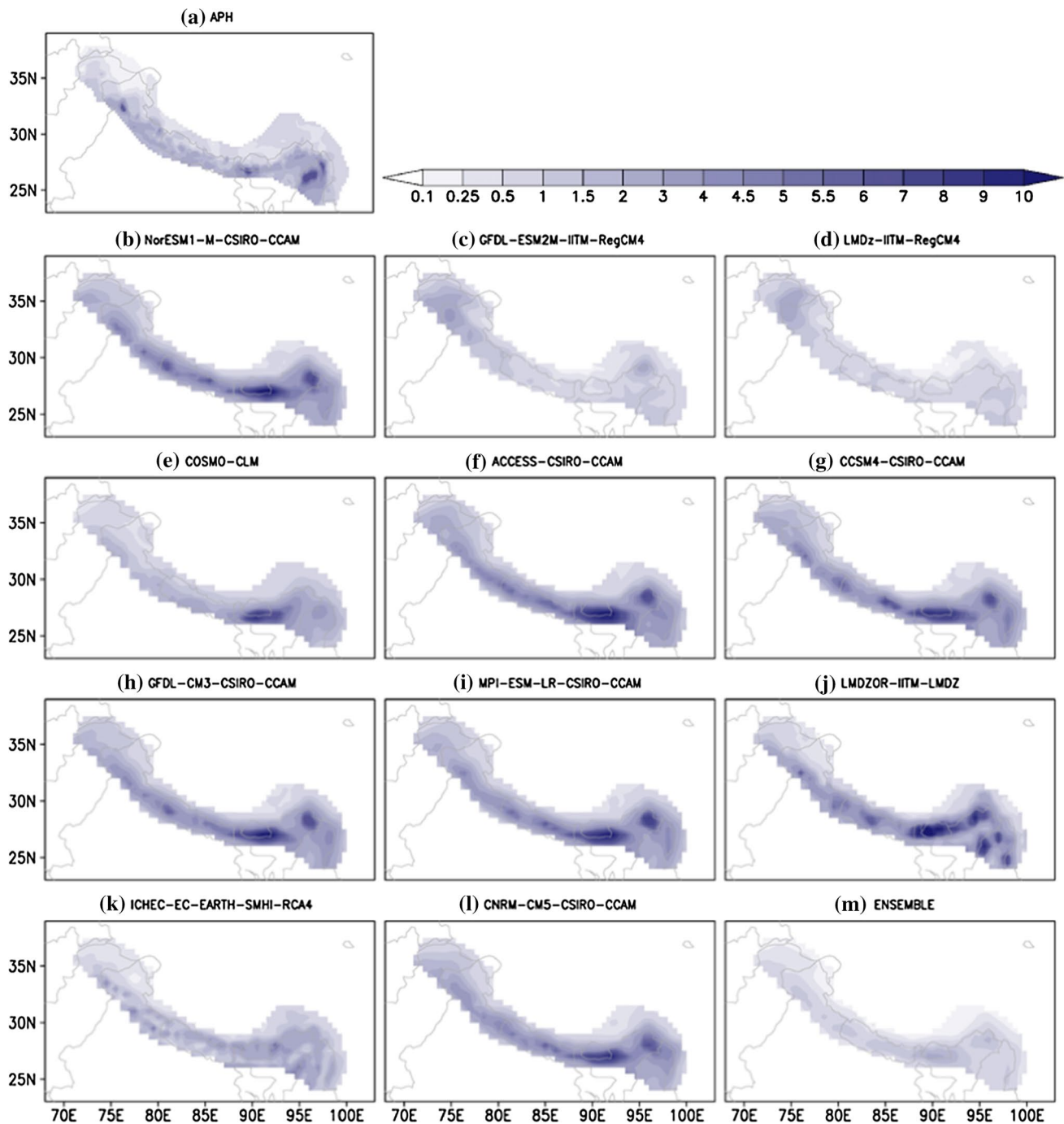


Fig. 8 a Standard deviation (mm/day) for observation and (b–m) same as Fig. 4, but for standard deviation of precipitation

for the same region an increasing trend of precipitation of over 0.1 mm/day/year is noted. Most noticeably, for the Karakoram region the two experiments in Fig. 9c and h are well in agreement with the observation capturing the trend at least the sign of increase if not the magnitude. A prominently observed feature in the experiments is that LMDZ-IITM-RegCM4 in Fig. 9d is showing an increasing trend for almost whole region though the values are very small. For

the ensemble mean of the experiments (Fig. 9m) the trend values are much less because of the cancellation of opposite signed values of yearly monsoonal mean precipitation of individual experiments and also smaller spatial variability is seen as decreasing trend is found in western half of the region and opposite in the eastern half. The spatially averaged time series of precipitation show an increasing trend for 4 experiments out of 11 while rest shows a drying trend

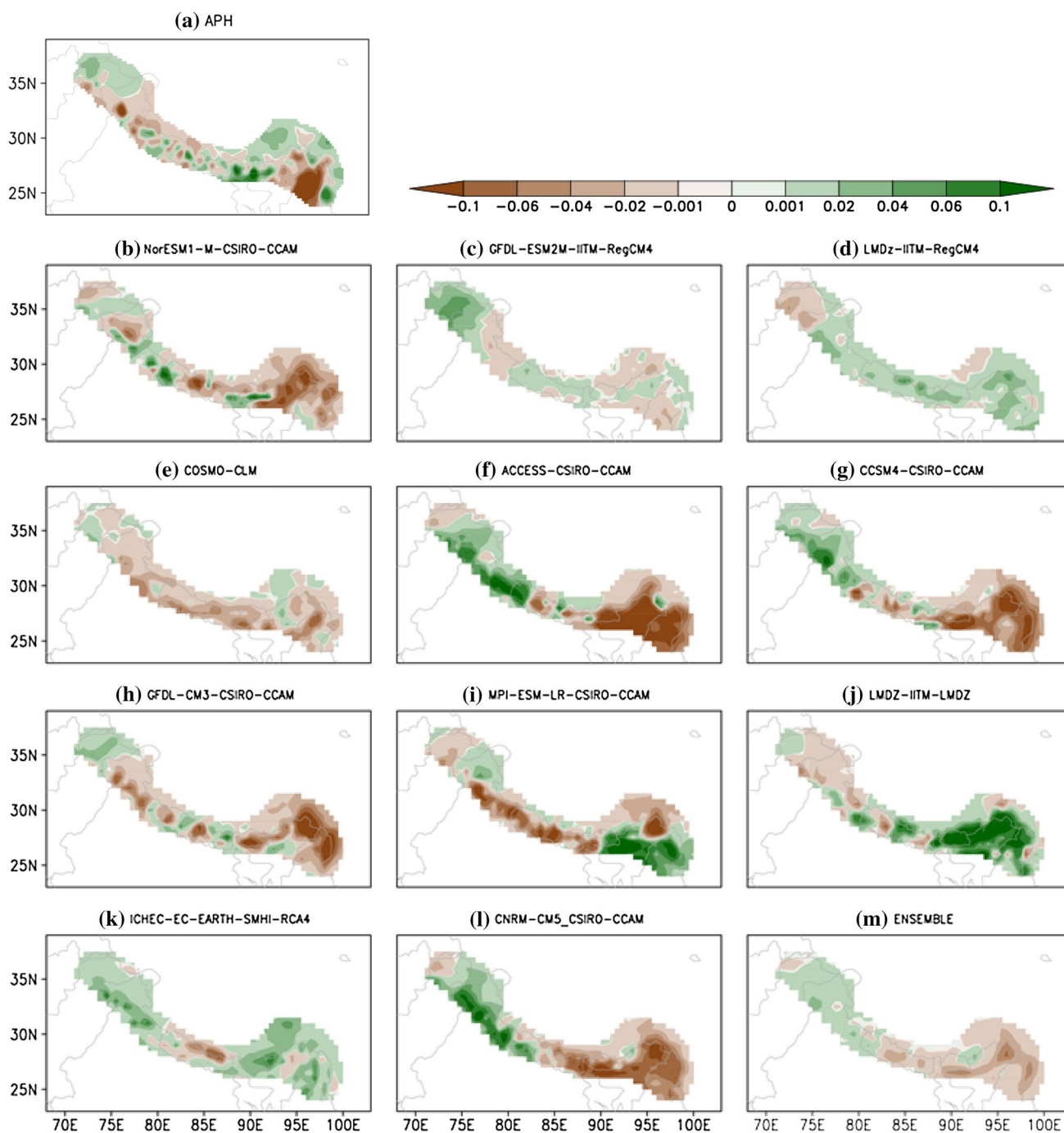


Fig. 9 Same as Fig. 8, but of JJAS precipitation trend (mm/day/year)

but it is important to mention here that trends of none of the experiments are statistically significant. In general, the experiments among themselves as well as compared with the observation vary substantially in simulating the trend and its distribution for 1970–2005 monsoon precipitation with only one experiment COSMO-CLM showing some signs of spatially consistent agreement of trend simulation. The inability of the experiments in simulating the observed

trend could be due to misrepresentation of local feedbacks in the model physics (e.g., Pal and Eltahir 2003) or poor representation of some atmospheric constituents like aerosol (Palazzi et al. 2013) which substantially contributes to the simulated variability and trends in the precipitation. For e.g. soil moisture and precipitation can interact at regional scales to significantly affect the regional precipitation trends and patterns (Giorgi et al. 2004).

The temporal pattern or variation of the yearly JJAS mean precipitation averaged over the study region for the given time period of 36 years (1970–2005) is shown in Fig. 10a. It shows the absolute value of precipitation for each year from 1970 to 2005 for all the experiments, ENS and APH. Here, the maximum precipitation of 10.1 mm/day is observed from the NorESM in the year 1978 and minimum precipitation of 2.98 mm/day in 1993 is shown by LMDZ-RegCM4. Only for the experiment ICHEC the range of precipitation values (5.61–8.82 mm/day) over the study period resembles to a moderately sufficient degree to that of APH (4.1–6.34 mm/day). While most of the other experiments show a consistent wet bias against APH. ENS is able to capture the precipitation pattern closer to APH, due to the cancellation of opposite signs in bias existing in individual experiments and thus shows improved performance compared to the individual experiments.

The uncertainty among the experiments is shown spatially in the Fig. 10b. It shows the spatial distribution of the spread in precipitation among the experiments over the study area. The spread among the experiments is calculated at each grid point as the standard deviation of the 36 year mean of each experiment with that of their ENS. Here we can see, there is a considerable spread among the experiments in the areas where higher precipitation (see Fig. 4) was seen in general for most of the experiments. This means the different models are simulating the process responsible for high precipitation but the magnitudes differ substantially between them due to difference in their physics or schemes to represent such processes associated with generating heavy precipitation. A larger spread is seen all along the central section of the study area spanning from 75°E to 96° E. While the western most regions over Hindu-Kush Himalaya and the entire peripheral stretch of the study region show smaller spread. In addition, the uncertainty is also shown in Fig. 10c through the spread in the area averaged JJAS mean precipitation of the experiments which is calculated for each year to show its variation. The spread of precipitation is ranging from maximum up to 10.1 mm/day, and minimum up to be as less as 2.98 mm/day and the average is obtained to be 7.04 mm/day. The standard deviation of JJAS precipitation averaged over the region shows the spread of the 11 experiment simulations from the ENS for different years over the given time period. However, peaking of precipitation is seen in accordance with the corresponding observation.

Figure 10d shows the mean of APH along with ± 3 standard deviation, to select better performing experiments. To identify the better performing experiment we have considered only the climatology, taking into account the spatial distribution and the long term mean of precipitation. Though there can be other ways to find out the better performing experiments by analyzing the dynamics of each

one of them. However, it is beyond the scope of the present study as we are mainly focusing only to study about the precipitation and uncertainty among the experiments. It has been clearly seen that the JJAS precipitation simulated by only one experiment ICHEC lies within the ± 3 variation from the mean. The selection of experiment was carried out based on its performance over the region for the given time period. Despite of the fact that the means of all the experiments deviate away from the APH mean, however their ENS lies close to the $+3$ standard deviation.

After choosing ICHEC as the better performing experiment, the assessment of the consistency of the experiment and ENS in simulating the spatial distribution of observed precipitation (JJAS mean) over time (1970–2005) was analyzed by the calculation of spatial correlation. The temporal correlation was also computed to determine how well the experiment is able to represent with spatial consistency the observed temporal variability of precipitation over the 36 years study period. Figure 11a depicts the magnitude and variability of the spatial correlations with the ICHEC experiment and the ENS with the observation. In general, ICHEC experiment and the ENS show inconsistency in representing spatial distribution of the precipitation over the years. Also the correlations values are not good except for ENS where for some years the values are above 0.6 which can be considered to be good up to a extent. The least correlation for the ICHEC was obtained to be 0.39 during 2002 and maximum of 0.57 during 1985. Similarly for ENS the minimum was obtained to be 0.50 in the year 1979 and maximum was 0.67 for 2003. Figure 11b, c which presents the spatial distribution of temporal correlation of for ICHEC experiment and ENS with the corresponding APH observation show that negative correlations are found at most of the places in the ICHEC experiment with correlations occasionally reaching up to 0.6 at a few places. This represents the poor capture of the year to year change in the precipitation by the experiment. This was also evident in the temporal variability analysis earlier discussed (see Fig. 10a). The ENS also shows similar kind of inconsistency with no good correlation across the study area.

The ability of the experiments to simulate the spatial pattern of JJAS mean precipitation is shown by the Taylor diagram, which provides a way of summarizing how closely the experiments match with the observation. Figure 12a shows the pattern correlation, RMS difference and the standard deviation of the seasonal mean precipitation of the experiments and ENS with respect to APH. The experiment COSMO shows higher pattern correlation of 0.8 with APH compared to other experiments. ENS, ICHEC and COSMO are able to capture the spatial variability to a good extent as evident from their closer standard deviations value to that of APH. In another sense it indicates that the pattern variations are of the right amplitude (Taylor 2005). ICHEC

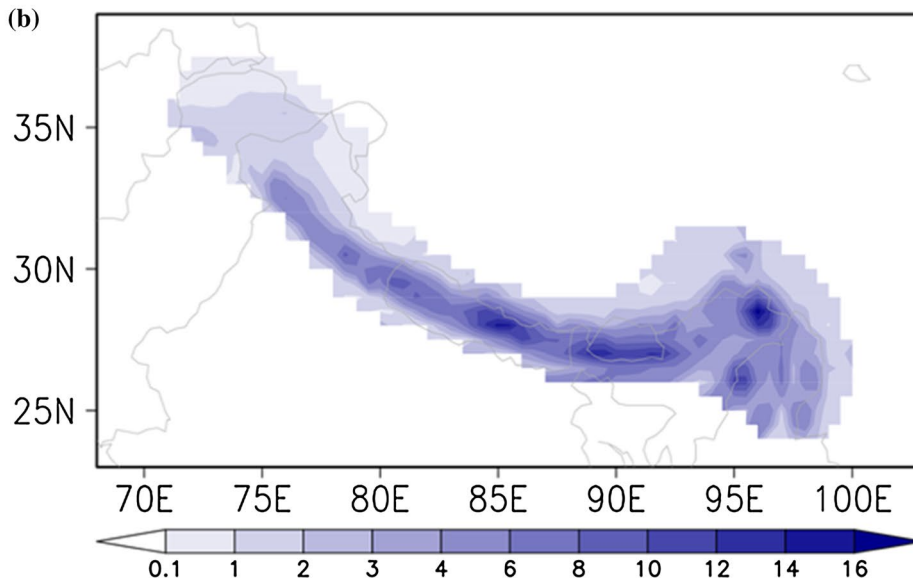
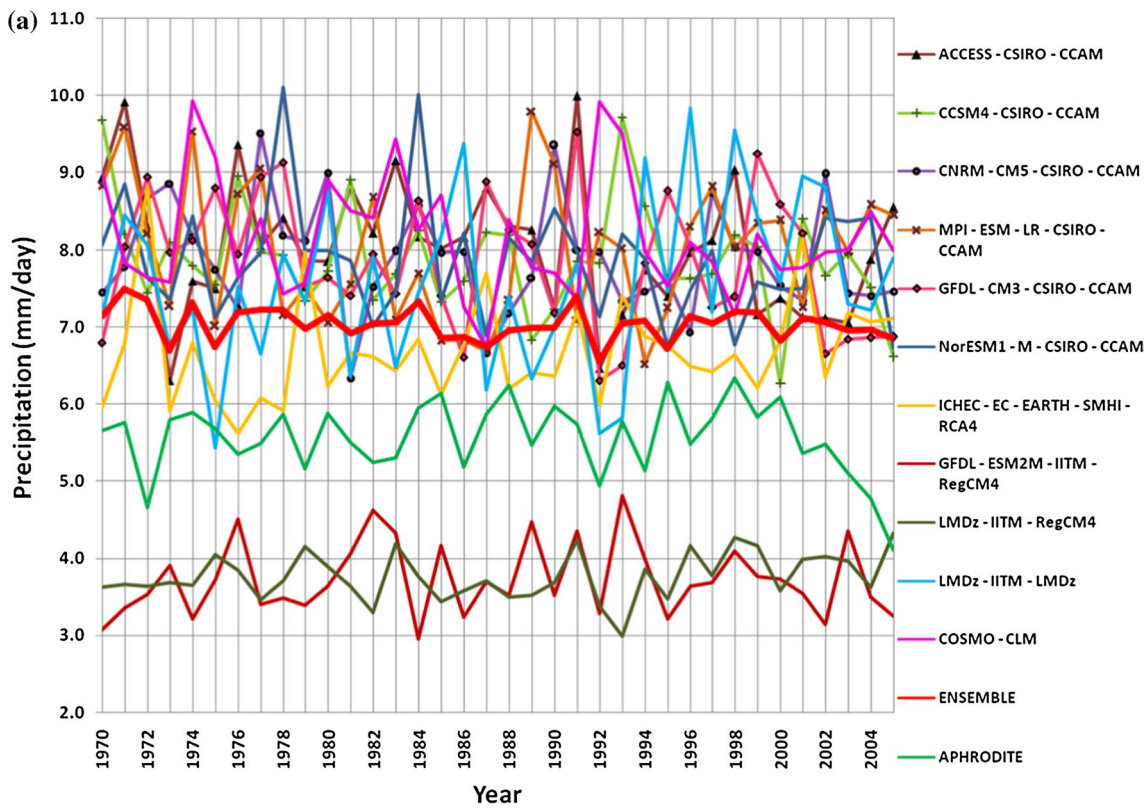


Fig. 10 **a** Time series of seasonal JJAS precipitation (mm/day) of 11 CORDEX experiments, their ensemble and the corresponding observation averaged over the study region (Fig. 1b), **b** standard deviation of precipitation (mm/day) for 1970–2005 over the study area for 11 experiments, **c** temporal plot of ensemble spread among the 11 CORDEX experiments during JJAS precipitation (mm/day) averaged over the study area. The ensemble is shown by the red line, the ± 1 SD of the ensemble is denoted with the purple bars and the minimum and the maximum values among all the 11 CORDEX experiments are

shown by the shaded region as well as by the whisker plots, whereas the blue line shows the observation APHRODITE data and **d** precipitation (mm/day) analysis between 11 CORDEX experiments and corresponding observation. The thick black line denotes the mean precipitation (mm/day) of the observation, the dashed lines represent the ± 3 SD of the mean of the observation, the dots represent the mean of each CORDEX experiments and the whisker bars associated to each dot are the ± 1 SD of the mean of each experiments

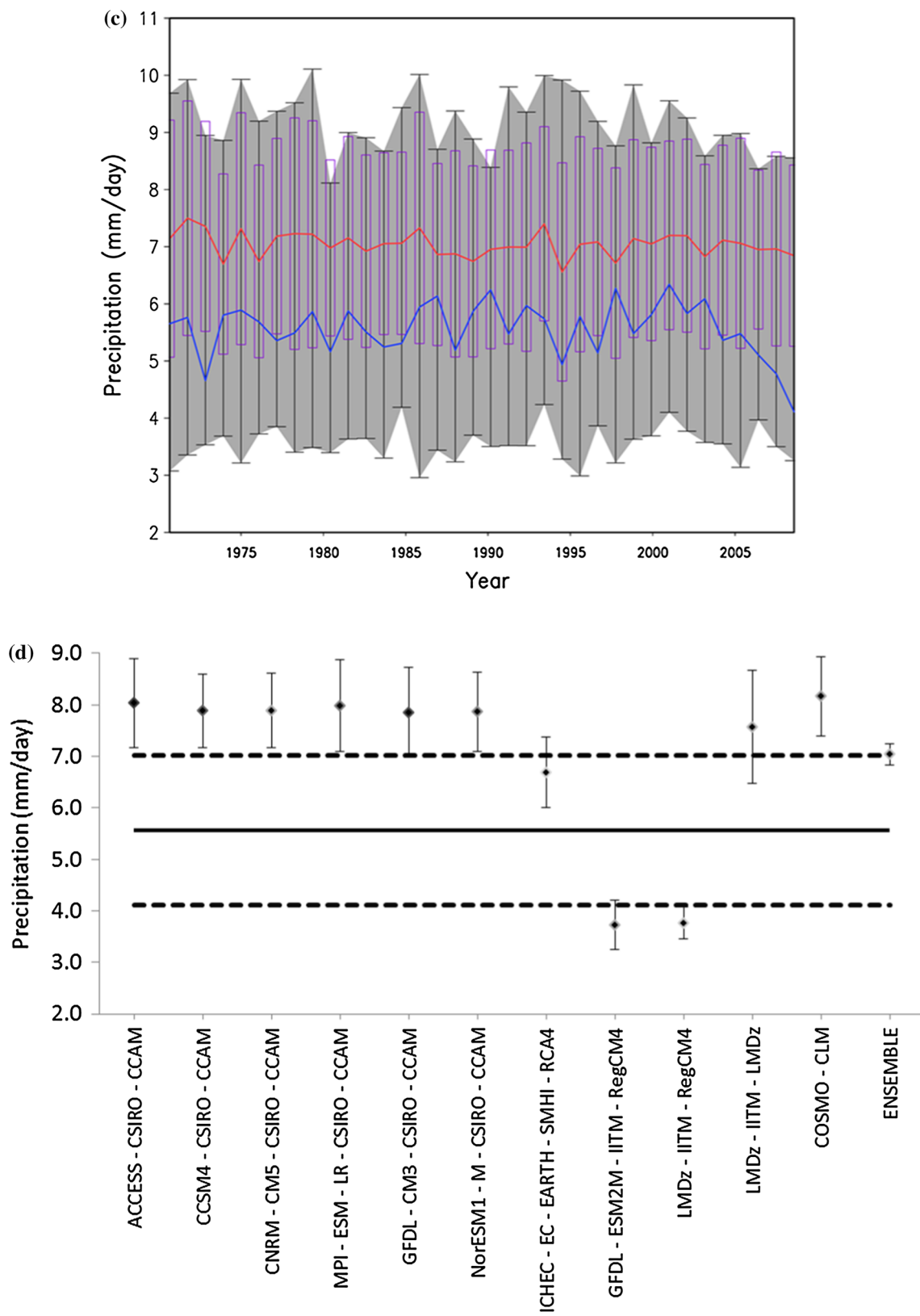


Fig. 10 continued

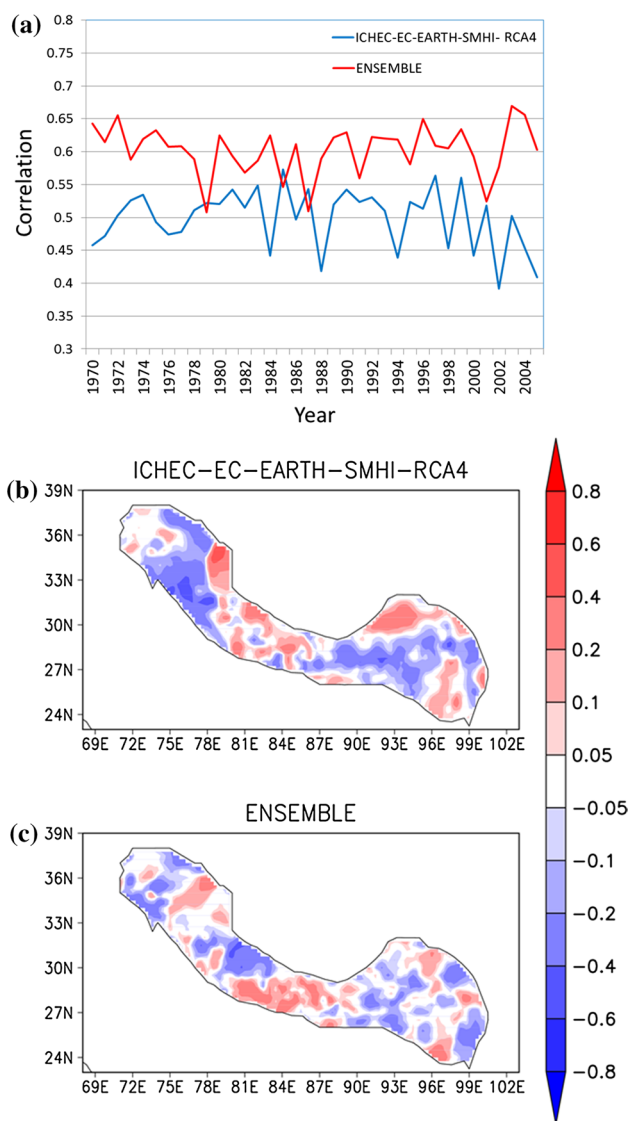


Fig. 11 a Spatial correlation of the JJAS precipitation (mm/day) between the ICHEC and ensemble with corresponding observation, b temporal correlation of JJAS precipitation (mm/day) from 1970 to 2005 of ICHEC with the corresponding observation and c similarly, temporal correlation of ENS with the corresponding observation

and ENS show pattern correlation approximately equal to 0.6. Therefore, we conclude that the patterns simulated by ICHEC, COSMO and ENS agree well with the APH, as indicated by closer standard deviation value to that of APH, lower RMS error and higher correlation compared to other experiments. However, GFDL-ESM2M and LMDZ-RegCM4 though show smaller RMS error and correlation similar to ICHEC, but both the experiments show much lower standard deviation when compared with APH indicating their poor ability in simulating the spatial variability of precipitation. Rest of the other seven experiments—the ones which use CCAM model for downscaling (S. no. 3–8;

Table 1) and another LMDZ show poor performance on Taylor diagram parameters as they produce higher standard deviation, higher RMS error and smaller correlation with APH. The resemblances/associations in the mean JJAS precipitation of the experiment ICHEC and ENS with the APH is presented in Fig. 12b in form of scatter plot. It shows that the mean precipitation is mostly concentrated within the range of 5–10 mm/day. More the data points are closer to the diagonal line, more they match closely with the APH value. It is clearly seen that the JJAS mean precipitation for ICHEC are more scattered compared to that of the ENS. Below 10 mm/day of precipitation intensity ICHEC shows good association with APH while for higher values the error increases on both sides of zero difference line or the diagonal, similar is the case with ENS. This may point towards the inherent weakness in the models to simulate the higher precipitation events.

The spatial distribution of seasonal mean precipitation and its annual cycle does not give a complete picture of the behaviour and strength or shortcomings of the experiments. Therefore, an evaluation and debate on the frequency distribution of precipitation against the corresponding observation has been made to assess and better understand the ability of the experiments in reproducing the spatial variability of precipitation intensity in a more comprehensible manner. Besides understanding the capability of the experiments in describing the entire range and frequencies of precipitation it also allows evaluating whether the RCMs are able to capture the occurrence of extreme precipitating events (Tapiador et al. 2007; Kjellstrom et al. 2010). This analysis will also come into frame in estimating a degree of certainty in making projections of climate change based on the future period data of these experiments, especially related with the projected changes in the occurrences of extreme events. For understanding the frequency distribution of the ENS, the best selected experiment (ICHEC) and the corresponding observation (APH), the value of JJAS mean precipitation intensity at each grid point (a single value as time average over the study period) was taken and their percentage frequency was calculated (see Table 3 and related Fig. 12c) for the entire range of values with bin widths of 1 mm/day. The Fig. 12c also shows the probability distribution function as gamma distribution curve. ICHEC and ENS show higher mean value (as suggested by location parameter, μ) and the standard deviation (σ) than the corresponding observation. When compared with ICHEC, ENS shows a higher difference from APH in its shape parameter, α indicating the former's (ICHEC) closer resemblance in shape with APH and hence in the frequency distribution also. This is further strengthened by the fact that curve of ENS with its scale parameter, β being much higher than APH compared with that of ICHEC suggests a squeeze in the curve and a larger discrepancy from observation in representing

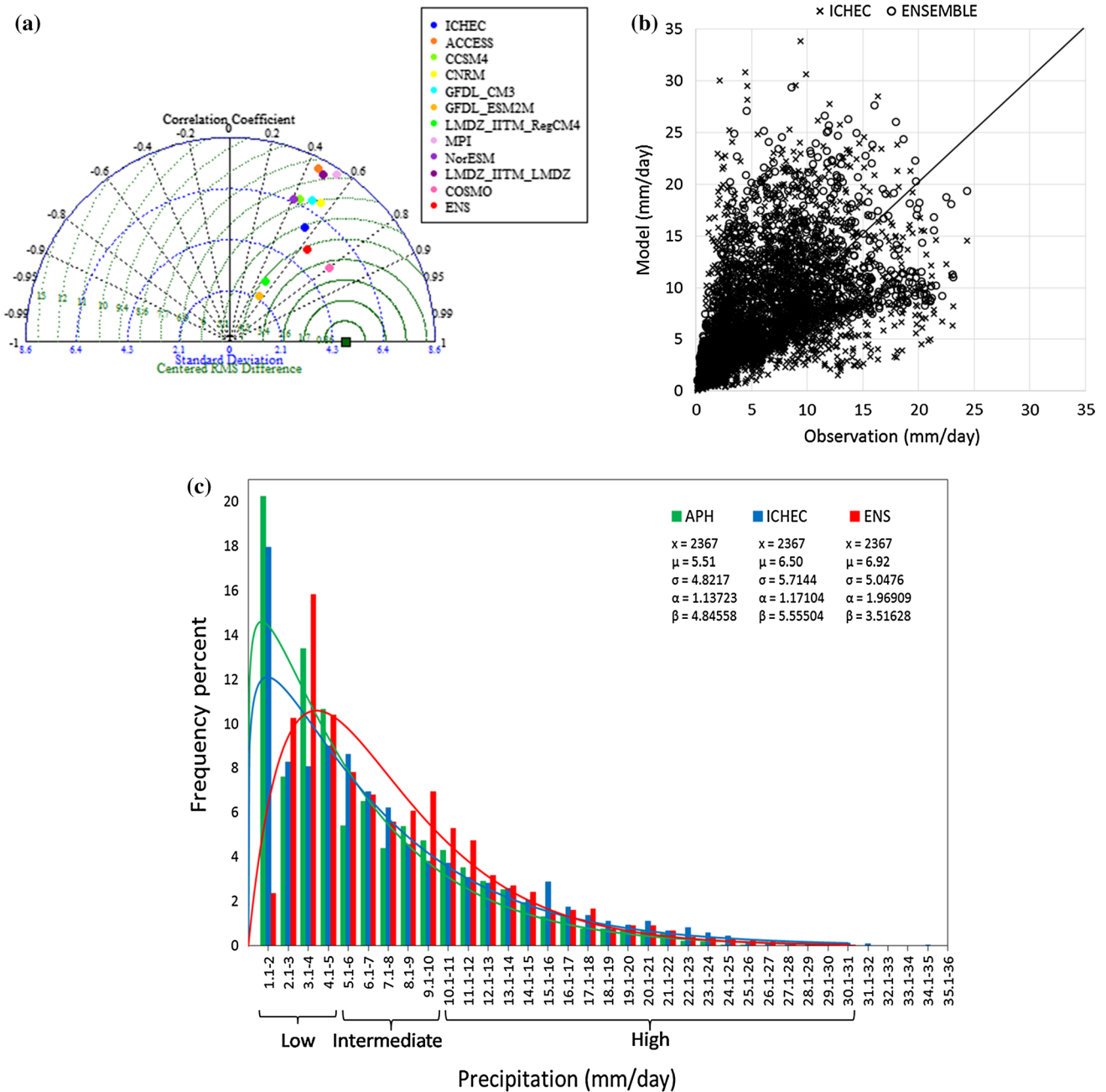


Fig. 12 **a** Taylor diagram showing statistical comparison of seasonal mean precipitation (mm/day) from 1970 to 2005 of the 11 CORDEX experiments, their ensemble and the observation (APH), **b** scatter plot showing the scatter spread of the precipitation (mm/day) of the ICHEC and ensemble with respect to the observation and **c** probability distribution function showing percentage of precipitation data fall-

ing within a particular range (in bar) and gamma distribution (in line) where ‘x’ is the no. of grid points in the study area; ‘ σ ’ is the standard deviation over area and μ , α and β are respectively, the location, shape and scale parameters of the gamma distribution. The range has been classified into low, intermediate and high based upon respectively $+1\sigma$, $+2\sigma$ and $+3\sigma$ of the observation

the distribution of precipitation intensities. The observed frequency distribution i.e. APH is characterized by a narrow curve with most of the precipitation concentrated in the low range and the peak lies in the range of 1.1–2 mm/day. As seen in Table 3 and suggested from the distributions of ICHEC and ENS which is the mean of all experiments,

most of the experiments in general except for a few ranges in lower side may be overestimating the frequency over the entire range of precipitation indicating a presence of systematic precipitation bias in the model output. This may be due to weaknesses in either the convection scheme or cloud microphysics scheme used in the models and could

Table 3 Range of the summer monsoon precipitation (mm/day) and its corresponding frequency for APH, ICHEC and ENS

	Range	Percentage frequency		
		APH	ICHEC	ENS
Low (based on $+1\sigma$ of the observation)	0.1–1	0	0.04	0
	1.1–2	20.24	17.96	2.37
	2.1–3	7.60	8.28	10.27
	3.1–4	13.39	8.07	15.84
	4.1–5	10.65	9.00	10.39
Intermediate (based on $+2\sigma$ of the observation)	5.1–6	5.41	8.62	7.82
	6.1–7	6.51	6.93	6.80
	7.1–8	4.39	6.21	5.58
	8.1–9	5.37	4.56	6.08
	9.1–10	4.73	3.80	6.93
High (based on $+3\sigma$ and higher of the observation)	10.1–11	4.31	3.72	5.28
	11.1–12	3.51	3.08	4.73
	12.1–13	2.92	2.83	3.17
	13.1–14	2.53	2.58	2.70
	14.1–15	1.94	2.07	2.41
	15.1–16	1.31	2.87	1.56
	16.1–17	1.35	1.73	1.61
	17.1–18	0.76	1.35	1.65
	18.1–19	0.76	1.10	0.72
	19.1–20	0.68	0.93	0.89
	20.1–21	0.63	1.10	0.89
	21.1–22	0.55	0.68	0.68
	22.1–23	0.21	0.80	0.38
	23.1–24	0.17	0.59	0.38
	24.1–25	0.04	0.42	0.25
	25.1–26	0.04	0.13	0.25
26.1–27	0	0.13	0.17	
27.1–28	0	0.04	0.08	
28.1–29	0	0.04	0.08	
29.1–30	0	0.08	0	
30.1–31	0	0.13	0.04	

be related to misrepresentation of clouds or even surface fluxes. Such systematic biases if exists could be removed through bias correction methods. Furthermore, the ICHEC and ENS show a longer tail than the observation APH indicating an overestimation of the spatial variability. Also for very high precipitation ranges the ICHEC and ENS show smaller variation from APH and in better agreement with each other compared with that in low range. From this plot, we can clearly see that both ICHEC and ENS are able to represent the log-normal shape—a characteristic feature of the precipitation distribution with APH and ICHEC in general, showing higher frequencies of precipitations in the low to mid-intermediate ranges whereas ENS is showing higher frequencies of precipitations in the intermediate

range which also persists towards high ranges up to a extent. For most of the high precipitation ranges above 15 mm/day ICHEC again tops but with slight difference. The analysis of biases in the individual models by studying their frequency distributions could be very useful for applying the proper bias correction methodologies.

4 Conclusions

The study of the precipitation climatology over the Himalayan region is a very complex task, due to heterogeneous and variable topography. Also, the precipitation over the Himalayan region is highly influenced by both ISM and WD. The precipitation patterns widely vary as the moist-laden clouds move along and across the Himalaya with orographic interaction between the two. The convection is affected due to the sudden and uninterrupted range of Himalaya. Due to sparse rain gauges and station, sufficient data cannot be attained which makes it difficult to evaluate the precipitation climatology, hence this has to be done only with the help of gridded dataset including models and observation.

In this study the performance of 11 CORDEX South Asia experiments was evaluated for their ability to capture and characterize the precipitation climatology over the Himalayan region for the time period of 36 years from 1970 to 2005 representing the present climate. The study was targeted in assessing the performance of the individual experiments and their ensemble. The performance of experiments was evaluated with respect to the corresponding observation. APH was chosen as the observational dataset for showing better result in the study region and for the fact that it incorporates the vertical interpolation of data, which is essential for the complex topography. In general, the experiments have performed well in capturing the precipitation in certain areas of the study domain, especially in the lower elevation. However, almost all of the experiments show wet bias against the observation consistently over time as also seen in the simulations of annual cycle of precipitation. But interestingly, dry bias is found over eastern Himalaya. We can refer this dry bias as underestimation of precipitation by the experiments in eastern Himalaya. Such biases could be related to the weaknesses in the model physics or even the error in the observation both of which needs to be improved in order to have reliable simulations for future climate. In further analysis of bias it was found that the biases in the experiments vary with elevation also with most of the experiments in general showing a positive bias in middle elevations and negative biases in lower elevations while for higher elevations the experiments performed well as indicated by smaller biases.

The experiments show wide variation among themselves and over time and space in simulating the precipitation over the study region as found from the uncertainty analysis. However, speaking in overall sense, ENS shows better performance compared to the individual experiments, due to cancellation of the opposite biases. Both the experiments and the ENS shows negative correlation and inconsistency with the observation in representing the year to year changes in the variability of precipitation as evident from time series as well as spatial distribution of temporal correlation and standard deviations. However, interestingly, all the experiments are able to capture the spatial variability in the precipitation up to some extent with a certain consistency over the entire study period as seen in the spatial correlation diagram.

Regional climate models tend to show biases in the region of complex topography throughout the world and these biases may get exaggerated for the reason that the observations have their own inaccuracies and uncertainties due to lack of dense observational networks (Walker and Diffenbaugh 2009; Nikulin et al. 2011). Only one experiment (ICHEC) was chosen for its better performance compared to other experiments and its close proximity with the observational dataset. The overall performance of the experiments showed wet bias with the observational dataset, consistently over time and space. Such bias in the models can be removed by bias correction to improve the accuracy of the models output. Further, from the frequency distribution analysis we clearly see that both ICHEC and ENS are able to represent the log-normal shape—a characteristic feature of the precipitation distribution. Moreover, the distributions of ICHEC and ENS which is the mean of all experiments, suggest that most of the experiments in general except for a few ranges in lower side may be overestimating the frequency over the entire range of precipitation indicating a presence of systematic precipitation bias in the model output. The analysis of biases in the individual models in such ways could be very useful for applying the proper bias correction methodologies (Li et al. 2010; Piani et al. 2010). This could be the future scope of this work.

Though no attempt has been made in the present study to understand the reasons behind the shortcomings and disagreements in the models but the knowledge generated from this study which documents the performance of 11 experiments—their common strength and major weaknesses, at one place may be informative to select individual models and improve them in order to increase the reliability of the CORDEX experiments for future projections of precipitation over this region which is very vulnerable to climatic changes.

Acknowledgments The authors thank World Climate Research Programme's Working Group on Regional Climate, and the

Working Group on Coupled Modelling and Center for Climate Change Research (CCCR), Indian Institute of Tropical Meteorology for provision of CORDEX South Asia data. Also, we thank Ministry of the Environment, Japan for APH's water resources project, supported by the Environment Research and Technology Development Fund. We are also grateful to two anonymous reviewers for making important comments and suggestions in improving the manuscript.

References

- Andermann C, Bonnet S, Gloaguen R (2011) Evaluation of precipitation data sets along the Himalayan front. *Geochem Geophys Geosyst* 12(7)
- Anders AM, Roe GH, Hallet B, Montgomery DR, Finnegan NJ, Putkonen J (2006) Spatial patterns of precipitation and topography in the Himalaya. *Geol Soc Am* 398:39–53
- Archer DR, Fowler HJ (2004) Spatial and temporal variations in precipitation in the Upper Indus Basin, global teleconnections and hydrological implications. *Hydrol Earth Syst Sci* 8(1):47–61
- Bajracharya SR, Mool PK, Shrestha BR (2007) Impact of climate change on glaciers and glacial lakes. International Center for Integrated Mountain Development, Kathmandu
- Bolch T, Kulkarni A, Kääb A, Huggel C, Paul F, Cogley G, Frey H, Kargel JS, Fujita K, Scheel M, Bajracharya S, Stoffel M (2012) The state and fate of Himalayan glaciers. *Science* 336:310–314
- Bookhagen B, Burbank DW (2006) Topography, relief, and TRMM-derived rainfall variations along the Himalaya. *Geophys Res Lett* 33(8)
- Bookhagen B, Burbank DW (2010) Toward a complete Himalayan hydrological budget: spatiotemporal distribution of snowmelt and rainfall and their impact on river discharge. *J Geophys Res: Earth Surface* (2003–2012), 115(F3)
- Dash SK, Sharma N, Pattanayak KC, Gao XJ, Shi Y (2012) Temperature and precipitation changes in the north-east India and their future projections. *Glob Planet Change* 98:31–44
- Denis B, Laprise R, Caya D, Cote J (2002) Downscaling ability of one-way nested regional climate models: the Big-Brother experiment. *Clim Dyn* 18:627–646
- Dimri AP (2004) Impact of horizontal model resolution and orography on the simulation of a western disturbance and its associated precipitation. *Meteorol Appl* 11(2):115–127
- Dimri AP (2009) Impact of subgrid scale scheme on topography and landuse for better regional scale simulation of meteorological variables over western Himalayas. *Clim Dyn* 32(4):565–574
- Dimri AP, Mohanty UC (2009) Simulation of mesoscale features associated with intense western disturbances over western Himalayas. *Meteorol Appl* 16(3):289–308
- Dimri AP, Niyogi D (2012) Regional climate model application at subgrid scale on Indian winter monsoon over the western Himalayas. *Int J Climatol* 33(9):2185–2205
- Dimri AP, Yasunari T, Wiltshire A, Kumar P, Mathison C, Ridley J, Jacob D (2013) Application of regional climate models to the Indian winter monsoon over the western Himalayas. *Sci Total Environ* 468:S36–S47
- Dimri AP, Niyogi D, Barros AP, Ridley J, Mohanty UC, Yasunari T, Sikka DR (2015) Western disturbance: a review. *Rev Geophys*. doi:10.1002/2014RG000460
- Dobler A, Ahrens B (2008) Precipitation by a regional climate model and bias correction in Europe and South Asia. *Meteorol Z* 17:499–509
- Dufresne JL, Foujols MA, Denvil S, Caubel A, Marti O, Aumont O, Balkanski Y, Bekki S, Bellenger H, Benshila R, Bony S, Bopp L, Braconnot P, Brockmann P, Cadule P, Cheruy F, Codron F, Cozic A, Cugnet D, de Noblet N, Duvel JP, Ethé C, Fairhead L, Fichefet T, Flavoni S, Friedlingstein P, Grandpeix JY, Guez

- L, Guilyardi E, Hauglustaine D, Hourdin F, Idelkadi A, Ghattaas J, Joussaume S, Kageyama M, Krinner G, Labetoulle S, Lahellec A, Lefebvre MP, Lefevre F, Levy C, Li ZX, Lloyd J, Lott F, Madec G, Mancip M, Marchand M, Masson S, Meurdesoif Y, Mignot J, Musat I, Parouty S, Polcher J, Rio C, Schulz M, Swingedouw D, Szopa S, Talandier C, Terray P, Viovy N, Vuichard N (2013) Climate change projections using the IPSL-CM5 Earth System Model: from CMIP3 to CMIP5. *Clim Dyn* 40(9–10):2123–2165
- Dunne JP, John JG, Adcroft AJ, Griffies SM, Hallberg RW, Shevliakova E, Stouffer RJ, Cooke W, Dunne KA, Harrison MJ, Krasting JP, Malyshev SL, Milly PCD, Philipps PJ, Sentman LT, Samuels BL, Spelman MJ, Winton M, Wittenberg AT, Zadeh N (2012) GFDL's ESM2 global coupled climate-carbon Earth System Models. Part I: physical formulation and baseline simulation characteristics. *J Clim* 25(19):6646–6665
- Endris HS, Omondi P, Jain S, Lennard C, Hewitson B, Chang'a L, Awange JL, Dosio A, Ketiemi P, Nikulin G, Panitz HJ, Büchner M, Stordal F, Tazalika L (2013) Assessment of the performance of CORDEX regional climate models in simulating East African rainfall. *J Clim* 26(21):8453–8475
- Fasullo J, Webster PJ (2003) A hydrological definition of Indian monsoon onset and withdrawal. *J Clim* 16(19):3200–3211
- Fernández J, Fita L, García-Díez M, Gutiérrez JM (2010) WRF sensitivity simulations on the CORDEX African domain. In: EGU General Assembly Conference Abstracts. vol. 12, p 9701
- Flato G, Marotzke J, Abiodun B, Braconnot P, Chou SC, Collins W, Rummukainen M (2013) Evaluation of climate models. In: Climate change 2013: the physical science basis. Contribution of working group I to the fifth assessment report of the Intergovernmental Panel on Climate Change. Cambridge University Press, Cambridge, pp 741–866
- Fowler HJ, Archer DR (2006) Conflicting signals of climatic change in the Upper Indus Basin. *J Clim* 19(17):4276–4293
- Gao XJ, Shi Y, Zhang D, Wu J, Giorgi F, Ji Z, Wang Y (2012) Uncertainties in monsoon precipitation projections over China: results from two high-resolution RCM simulations. *Clim Res* 2:213–226
- Giorgetta MA, Jungclaus J, Reick CH, Legutke S, Bader J, Böttinger M, Brovkin V, Crueger T, Esch M, Fieg K, Glushak K, Gayler V, Haak H, Hollweg H-D, Ilyina T, Kinne S, Kornblueh L, Matei D, Mauritsen T, Mikolajewicz U, Mueller W, Notz D, Pithan F, Raddatz T, Rast S, Redler R, Roeckner E, Schmidt H, Schnur R, Segschneider J, Six KS, Stockhause M, Timmreck C, Wegner J, Widmann H, Wieners K-H, Claussen M, Marotzke J, Stevens B (2013) Climate and carbon cycle changes from 1850 to 2100 in MPI-ESM simulations for the Coupled Model Intercomparison Project phase 5. *J Adv Model Earth Syst* 5(3):572–597
- Giorgi F, Mearns LO (1999) Introduction to special section: regional climate modeling revisited. *J Geophys Res* 104:6335–6352
- Giorgi F, Shields Brodeur C, Bates GT (1994) Regional climate change scenarios over the United States produced with a nested regional climate model. *J Clim* 7(3):375–399
- Giorgi F, Bi X, Pal J (2004) Mean, interannual variability and trends in a regional climate change experiment over Europe. II: climate change scenarios (2071–2100). *Clim Dyn* 23(7–8):839–858
- Giorgi F, Jones C, Asrar GR (2009) Addressing climate information needs at the regional level: the CORDEX framework. *World Meteor Organ (WMO). Bulletin* 58(3):175
- Giorgi F, Coppola E, Solmon F, Mariotti L, Sylla MB, Bi X, Brankovic C et al (2012) RegCM4: model description and preliminary tests over multiple CORDEX domains. *Clim Res* 2(7)
- Hall G (2015) Pearson's correlation coefficient. http://www.hep.ph.ic.ac.uk/~hallg/UG_2015/Pearsons.pdf. Accessed 5 July 2015
- Hazeleger W, Wang X, Severijns C, Ștefănescu S, Bintanja R, Sterl A, Wyser K, Semmler T, Yang S, Van Der Hurk B, Noije T, Linden E, Van Der Wiel K (2012) EC-Earth V2.2: description and validation of a new seamless earth system prediction model. *Clim Dyn* 39:2611–2629
- Hirakuchi H, Giorgi F (1995) Multiyear present-day and 2x CO₂ simulations of monsoon climate over eastern Asia and Japan with a regional climate model nested in a general circulation model. *J Geophys Res* 100:21105–21125
- ICIMOD (2010) Climate change impact and vulnerability in the eastern Himalayas—synthesis report. International Center for Integrated Mountain Development, Kathmandu
- Immerzeel WW, Bierkens MF, Van Beek LP (2009) Hydrological response of climate change in a glaciated catchment in the Himalayas. In: AGU Fall meeting abstracts 1, 08
- Immerzeel WW, Van Beek LP, Bierkens MF (2010) Climate change will affect the Asian water towers. *Science* 328(5984):1382–1385
- IPCC (Intergovernmental panel on Climate Change) (2007) Climate change 2007: the physical sciences basis. In: Contribution of working group I to the fourth assessment report of the IPCC. Cambridge University Press, Cambridge
- Joshi S, Kumar K, Joshi V, Pande B (2014) Rainfall variability and indices of extreme rainfall—analysis and perception study for two stations over Central Himalaya, India. *Nat Hazards* 72(2):361–374
- Khan AR (2001) Analysis of hydro-meteorological time series: searching evidence for climatic change in the Upper Indus Basin. International Water Management Institute (IWMI), Pakistan, Lahore
- Kjellstrom E, Boberg F, de Castro M, Christensen JH, Nikulin G, Sanchez E (2010) On the use of daily and monthly temperature and precipitation statistics as a performance indicator for regional climate models. *Clim Res* 44:135–150
- Krishnamurti TN, Mishra AK, Simon A, Yatagai A (2009) Use of a dense gauge network over India for improving blended TRMM products and downscaled weather models. *J Meteorol Soc Jpn* 87:395–416
- Kulkarni A, Patwardhan S, Kumar KK, Ashok K, Krishnan R (2013) Projected climate change in the Hindu Kush-Himalayan region by using the high-resolution regional climate model PRECIS. *Mount Res Develop* 3(2):142–151
- Kumar V, Jain SK (2010) Trends in seasonal and annual rainfall and rainy days in Kashmir Valley in the last century. *Quat Int* 212(1):64–69
- Kumar V, Singh P, Jain SK (2005) Rainfall trends over Himachal Pradesh, Western Himalaya, India. In: Conference on development of hydro power projects—a prospective challenge, pp 20–22
- Kumar P, Wiltshire A, Mathison C, Asharaf S, Ahrens B, Lucas-Picher P, Christensen JH, Gobiet A, Saeed F, Hageman S, Jacob D (2013) Downscaled climate change projections with uncertainty assessment over India using a high resolution multi-model approach. *Sci Total Environ* 468:18–30
- Kumar P, Kotlarski S, Moseley C, Sieck K, Frey H, Stoffel M, Jacob D (2015) Response of Karakoram–Himalayan glaciers to climate variability and climatic change: a regional climate model assessment. *Geophys Res Lett* 42(6):1818–1825
- Laprise RRDE, De Elia R, Caya D, Biner S, Lucas-Picher P, Diaconescu E, Leduc M, Alexandru A, Separovic L (2008) Challenging some tenets of regional climate modelling. *Meteorol Atmos Phys* 100(1–4):3–22
- Li H, Sheffield J, Wood EF (2010) Bias correction of monthly precipitation and temperature fields from Intergovernmental Panel on Climate Change AR4 models using equidistant quantile matching. *J Geophys Res Atmos* (1984–2012) 115(D10)
- Mass C (1981) Topographically forced convergence in western Washington State. *Mon Weather Rev* 109(6):1335–1347
- Mathison C, Wiltshire A, Dimri AP, Falloon P, Jacob D, Kumar P, Moors E, Ridley J, Siderius C, Stoffel M, Yasunari T (2013)

- Regional projections of North Indian climate for adaptation studies. *Sci Total Environ* 468:S4–S17
- McGregor JL, Dix MR (2001) The CSIRO Conformal-Cubic Atmospheric GCM. In: Hodnett PF (ed) IUTAM symposium on advances in mathematical modelling of atmosphere and ocean dynamics. Kluwer, Dordrecht, pp 197–202
- Medina S, Houze RA, Kumar A, Niyogi D (2010) Summer monsoon convection in the Himalayan region: terrain and land cover effects. *Q J R Meteorol Soci* 136(648):593–616
- Mishra V (2015) Climatic uncertainty in Himalayan water towers. *J Geophys Res Atmos* 120(7): 2689–2705
- Mitchell TD, Jones PD (2005) An improved method of constructing a database of monthly climate observations and associated high-resolution grids. *Int J Climatol* 25(6):693–712
- Mukherjee S, Joshi R, Prasad RC, Vishvakarma SC, Kumar K (2014) Summer monsoon rainfall trends in the Indian Himalayan region. *Theor Appl Climatol* 1–14
- Nikulin G, Kjellström E, Hansson ULF, Strandberg G, Ullerstig A (2011) Evaluation and future projections of temperature, precipitation and wind extremes over Europe in an ensemble of regional climate simulations. *Tellus A* 63(1):41–55
- Nikulin G, Jones C, Giorgi F, Asrar G, Buchner M (2012) Precipitation climatology in an ensemble of CORDEX-Africa regional climate simulations. *J Clim* 25:6057–6078
- Pal JS, Eltahir EA (2003) A feedback mechanism between soil-moisture distribution and storm tracks. *Q J R Meteorol Soc* 129(592):2279–2297
- Palazzi E, Hardenberg J, Provenzale A (2013) Precipitation in the Hindu-Kush Himalaya: observations and future scenarios. *J Geophys Res* 118:85–100
- Pant GB, Borgeankar HP (1984) Climate of the hill regions of Uttar Pradesh. *Himal Res Dev* 3:13–20
- Pant GB, Rupa Kumar K, Borgeankar HP (1999) Climate and its long-term variability over the western Himalaya during the past two centuries. *The Himalayan environment*. New Age International (P) Limited, New Delhi, pp 171–184
- Piani C, Haerter JO, Coppola E (2010) Statistical bias correction for daily precipitation in regional climate models over Europe. *Theor Appl Climatol* 99(1–2):187–192
- Rajbhandari R, Shrestha AB, Kulkarni A, Patwardhan SK, Bajracharya SR (2014) Projected changes in climate over the Indus river basin using a high resolution regional climate model (PRECIS). *Clim Dyn* 44(1–2):339–357
- Rasmussen R, Baker B, Kochendorfer J, Meyers T, Landolt S, Fischer AP, Gutmann E et al (2012) How well are we measuring snow: the NOAA/FAA/NCAR winter precipitation test bed. *Bullet Amer Meteorol Soci* 93(6):811–829
- Roe GH (2005) Orographic precipitation. *Annu Rev Earth Planet Sci* 33:645–671
- Rudolf B, Becker A, Schneider U, Meyer-Christoffer A, Ziese M (2011) New GPCC full data reanalysis version 5 provides high-quality gridded monthly precipitation data. *Gewex News* 21(2):4–5
- Rummukainen M (2010) State-of-the-art with regional climate model. *Wiley Interdiscip Rev Clim Change* 1:82–96
- Sabin TP, Krishnan R, Ghattas J, Denvil S, Dufresne JL, Hourdin F, Pascal T (2013) High resolution simulation of the South Asian monsoon using a variable resolution global climate model. *Clim Dyn* 41(1):173–194
- Samuelsson P, Jones CG, Willén U, Ullerstig A, Gollvik S, Hansson U, Jansson C, Kjellström E, Nikulin G, Wyser K (2011) The Rossby Centre Regional Climate model RCA3: model description and performance. *Tellus A* 63(1):4–23
- Schneider U, Becker A, Finger P, Meyer-Christoffer A, Rudolf B, Ziese M (2011) GPCC full data reanalysis version 6.0 at 0.5: monthly land-surface precipitation from rain-gauges built on GTS-based and historic data. doi:10.5676/DWD_GPCC.FD_M_V6_050
- Schulzweida U, Kornblueh L, Quast R (2006) CDO user's guide. *Clim Data Oper*. Version 1(6)
- Sharma KP, Moore Iii B, Vorosmarty CJ (2000) Anthropogenic, climatic, and hydrologic trends in the Kosi Basin, Himalaya. *Clim Change* 47(1–2):141–165
- Shi Y, Gao X, Zhang D, Giorgi F (2011) Climate change over the YarlungZangbo–Brahmaputra River Basin in the 21st century as simulated by a high resolution regional climate model. *Quat Int* 244(2):159–168
- Shrestha AB, Wake CP, Dibb JE, Mayewski PA (2000) Precipitation fluctuations in the Nepal Himalaya and its vicinity and relationship with some large scale climatological parameters. *Int J Climatol* 20(3):317–327
- Singh P, Kumar N (1997) Effect of orography on precipitation in the western Himalayan region. *J Hydrol* 199(1):183–206
- Singh RB, Sen Roy S (2002) Climate variability and hydrological extremes in a Himalayan catchment. In: ERB and Northern European FRIEND project 5 Conference, Slovakia
- Singh S, Khadka BI, Karky B, Sharma E (2011) Climate change in the Hindu Kush Himalayas: the state of current knowledge. ICIMOD
- Sun L, Moncunill DF, Li H, Moura AD, Filho FD, Zebiak SE (2006a) An operational Dynamical downscaling prediction system for Nordeste Brazil and 2002–04 real time forecast evaluation. *J Clim* 19:1990–2007
- Sun Y, Solomon S, Dai A, Portmann RW (2006b) How often does it rain? *J Clim* 19:916–934
- Tapiador FJ, Sanchez E, Gaertner MA (2007) Regional changes in precipitation in Europe under an increased-greenhouse emissions scenario. *Geophys Res Lett* 34:L06701
- Taylor KE (2001) Summarizing multiple aspects of model performance in a single diagram. *J Geophys Res* 106(D7):7183–7192
- Taylor KE (2005) Taylor diagram primer. Program for Climate Model Diagnosis and Intercomparison. http://www.pcmdi.llnl.gov/about/staff/Taylor/CV/Taylor_diagram_primer.pdf. Accessed 5 July 2015
- Turk FJ, Arkin P, Sapiano MR, Ebert EE (2008) Evaluating high-resolution precipitation products. *Bull Am Meteorol Soc* 89(12):1911–1916
- Walker MD, Diffenbaugh NS (2009) Evaluation of high-resolution simulations of daily-scale temperature and precipitation over the United States. *Clim Dyn* 33(7–8):1131–1147
- Wang Y, Leung LR, Mcgregor JL, Lee DK, Wang WC, Ding Y, Kimura F (2004) Regional climate modeling: progress, challenges, and prospects. *J Meteorol Soci* 82(6):1599–1628
- WGMS (2008) Global glacier changes: facts and figures. UNEP
- Wilks DS (2011) Statistical methods in the atmospheric sciences, vol 100. Academic Press, San Diego
- Xie P, Chen M, Yang S, Yatagai A, Hayasaka T, Fukushima Y, Liu C (2007) A gauge-based analysis of daily precipitation over East Asia. *J Hydrometeorol* 8(3):607–626
- Yatagai A, Arakawa O, Kamiguchi K, Kawamoto H, Nodzu MI, Hamada A (2009) A 44-year daily gridded precipitation dataset for Asia based on a dense network of rain gauges. *Sci Online Lett Atmos* 5:137–140